NASA CONTRACTOR
REPORT

NASA CR-120558

(NASA-CR-120558) INDIUM ANTIMONIDE CRYSTAL GROWTH EXPERIMENT M562 Final Report (Massachusetts Inst. of Tech.) 80 p HC $4.75 CSCL 20B

N75-14907

Unclas
G3/27 06632

INDIUM ANTIMONIDE CRYSTAL GROWTH

Experiment M562

By Harry C. Gatos and August F. Witt
Massachusetts Institute of Technology
Cambridge, Massachusetts

September 1974

Final Report

Prepared for

NASA-GEORGE C. MARSHALL SPACE FLIGHT CENTER
Marshall Space Flight Center, Alabama 35812

TECHNICAL REPORT STANDARD TITLE PAGE

1. REPORT NO.	2. GOVERNMENT ACCESSION NO.	3. RECIPIENT'S CATALOG NO.
NASA CR-120558		

4. TITLE AND SUBTITLE
INDIUM ANTIMONIDE CRYSTAL GROWTH (M562)

5. REPORT DATE
September 1974

6. PERFORMING ORGANIZATION CODE

7. AUTHOR(S)
Harry C. Gatos and August F. Witt

8. PERFORMING ORGANIZATION REPORT #

9. PERFORMING ORGANIZATION NAME AND ADDRESS
Massachusetts Institute of Technology
Cambridge, Massachusetts

10. WORK UNIT NO.

11. CONTRACT OR GRANT NO.
NAS 8-28306

12. SPONSORING AGENCY NAME AND ADDRESS
National Aeronautics and Space Administration
Washington, D. C. 20546

13. TYPE OF REPORT & PERIOD COVERED
Contractor
Final

14. SPONSORING AGENCY CODE

15. SUPPLEMENTARY NOTES

16. ABSTRACT

It was established that ideal diffusion controlled steady state conditions, never accomplished on earth, were achieved during the growth of Te-doped InSb crystals in Skylab. Surface tension effects led to nonwetting conditions under which free surface solidification took place in confined geometry. It was further found that, under forced contact conditions, surface tension effects led to the formation of surface ridges (not previously observed on earth) which isolated the growth system from its container. In addition, it was possible, for the first time, to identify unambiguously: the origin of segregation discontinuities associated with facet growth, the mode of nucleation and propagation of rotational twin boundaries, and the specific effect of mechanical-shock perturbations on segregation.

The results obtained prove the advantageous conditions provided by outer space. Thus, fundamental data on solidification thought to be unattainable because of gravity-induced interference on earth are now within reach.

17. KEY WORDS	18. DISTRIBUTION STATEMENT
	Unclassified-unlimited James D. Ledbetter

19. SECURITY CLASSIF. (of this report)	20. SECURITY CLASSIF. (of this page)	21. NO. OF PAGES	22. PRICE
Unclassified	Unclassified	79	NTIS

TABLE OF CONTENTS

	Page
SUMMARY	v
GENERAL REMARKS	vi
OBJECTIVES	vi
ABSTRACT	1
INTRODUCTION	1
EXPERIMENTAL APPROACH	3
Crystal Growth Apparatus	3
Crystal Preparation and Assembly	4
Crystal Growth Procedure in Space	5
RESULTS AND DISCUSSION	6
MORPHOLOGICAL CHARACTERISTICS	7
Tellurium-Doped InSb Grown in Skylab-III	7
Tellurium-Doped InSb Grown in Skylab-IV	8
Bulk Characterization	10
Dopant Segregation	10
Quantitative Dopant Segregation Analysis	11
Intentionally Introduced Segregation Discontinuity	14
Crystal Morphology	16
Peripheral Facet Effect	17
Rotational Twinning	18
CONCLUSIONS	19
ACKNOWLEDGEMENTS	21
BIBLIOGRAPHY	22
APPENDIX A	A1
MATERIALS	
Indium Antimonide	A1
Dopant Elements and Doping Procedure	A1
Graphite	A1
Quartz	A2
Preparation of InSb Crystals Used for Ground-Based Testing and Skylab Experiments	A2

Table of Contents (continued)

	Page
APPENDIX B	B1
GROUND-BASED TESTING	B1
Characterization Procedures for Compositional Inhomogeneities on the Microscale	B1
Analysis of Growth and Segregation by Controlled Power Reduction in Confined Configuration	B3
Ground-Based Tests in the Prototype of the Multipurpose Furnace	B4
APPENDIX C	C1
SUPPLEMENTARY INFORMATION	C1

INDIUM ANTIMONIDE CRYSTAL GROWTH

SUMMARY

The analysis of the InSb crystals grown during the Skylab III and Skylab IV missions established unambiguously that ideal diffusion controlled steady state conditions, never achieved on earth in macroscopic dimensions, were attained during growth in the absence of gravitational forces. In addition, the results made it possible, for the first time, to identify: (a) the origin of segregation discontinuities associated with facet growth; (b) the mode of nucleation and propagation of rotational twin boundaries; (c) the effects of mechanical shock perturbation on dopant segregation. The experiments revealed, furthermore, that surface tension effects of the doping element are critical for the mode of solidification in confined geometry. Thus, it was found that the presence of tellurium dopant in Indium Antimonide led to non-wetting conditions between the melt and the quartz container; as a result, "free surface" solidification took place in a confined geometry. Under "forced contact" conditions, surface tension effects led to the formation of surface ridges (not previously observed on earth) which effectively isolated the growth system from its container. No evidence of bulk convection in the melt as predicted on the basis of the Marangoni effect (perturbations due to surface tension gradients) could be found in any crystal grown on Skylab. The quantitative analysis of the transition regions in the initial regrowth segments performed by Hall measurements and ion-microprobe measurements indicated that equilibrium segregation and solute diffusion data can readily be obtained from solidification experiments performed in the absence of gravity, provided the microscopic growth rate is known. The results of the InSb growth

experiments on Skylab demonstrate the unique advantages of gravity-free outer space on crystal growth and solidification in general.

GENERAL REMARKS

The salient results, obtained to date, are given in this final report essentially as presented at the Third Space Processing Symposium, Skylab Results, April 30-May 1, 1974, Marshall Space Flight Center, Alabama. Additional pertinent information on materials, results of ground-based tests, analytical procedures and techniques are presented in the form of appendices.

It is believed that further basic data will be obtained from the space-grown material as our understanding of solidification is advanced and more sensitive analytical techniques become available.

OBJECTIVES

The InSb crystal growth experiment (M-562) was conceived to study the following basic assumptions: (a) Crystal growth from the melt in the absence of gravitational forces takes place without thermal convection and results in exclusively diffusion controlled segregation; accordingly, steady state growth and segregation can be achieved in space and the resulting material should exhibit compositional homogeneity on the micro- and macroscale. (b) Fundamental, as yet not available, data on solidification can be obtained from the analysis of crystals grown under near zero gravity conditions; such data will help bridge the gap between theory and experiment and should lead toward optimization of materials processing technology which at present is based largely on empiricism.

It was also expected that the experiment would demonstrate any effects of surface tension forces on crystal growth and segregation, thought to be detrimental in the absence of gravitational forces.

The present experiment involved growth of undoped, Te-doped and Sn-doped InSb; it was designed to permit the direct comparison of the basic characteristics of growth on earth and in space by melting and resolidifying in space a portion of crystals grown on earth.

STEADY-STATE GROWTH AND SEGREGATION UNDER ZERO GRAVITY: InSb*

A. F. Witt, H. C. Gatos, M. Lichtensteiger,
M. C. Lavine, C. J. Herman
Massachusetts Institute of Technology
Cambridge, Massachusetts 02139

ABSTRACT

It was established that ideal diffusion controlled steady state conditions, never accomplished on earth, were achieved during the growth of Te-doped InSb crystals in Skylab. Surface tension effects led to non-wetting conditions under which free surface solidification took place in confined geometry. It was further found that, under forced contact conditions, surface tension effects led to the formation of surface ridges (not previously observed on earth) which isolated the growth system from its container. In addition, it was possible, for the first time, to identify unambiguously: the origin of segregation discontinuities associated with facet growth, the mode of nucleation and propagation of rotational twin boundaries, and the specific effect of mechanical-shock perturbations on segregation.

The results obtained prove the advantageous conditions provided by outer space. Thus, fundamental data on solidification thought to be unattainable because of gravity-induced interference on earth are now within reach.

INTRODUCTION

Structural and compositional control during solidification of materials is impeded by gravity-induced effects in the melt. Thermal gradients necessary for crystal growth lead, in the presence of gravitational forces, to

*Pages 1-24, as presented at the Third Space Processing Symposium, Skylab Results, April 30-May 1, 1974.

thermal convection which in general causes uncontrolled variations in the solidification rate and in diffusion boundary layer thickness; such variations lead directly to periodic and/or random microscopic and macroscopic segregation inhomogeneities. Furthermore, in the presence of gravity, establishing steep thermal gradients, often required to prevent constitutional supercooling, is impossible and consequently interface breakdown is unavoidable.

Gravity effects are, thus, primarily responsible for the present lack of reliable solidification data and the existing gap between theory and experiment. Consequently, crystal growth and associated segregation phenomena are still based on empiricism, and the properties and performance of solids are not at their theoretical limits.

Gravity-free conditions made accessible though the space program of NASA provide a unique opportunity to obtain reliable crystal growth data and, therefore, to advance our quantitative understanding of solidification processes; in addition this program makes possible the exploration and assessment of the potential of outer space for materials processing.

Indium antimonide was chosen for the presently reported Skylab experiment because its relatively low melting point (525°C) made the experiment compatible with the available electrical power. In addition, chemical etching, the only high-resolution technique available, at the time, for the study of segregation inhomogeneities on a microscale, had been developed on InSb to its most advanced level.

The experiments performed during the Skylab-III and -IV missions included the growth of undoped, tellurium-doped, and tin-doped indium antimonide. The present report is concerned primarily with results obtained on tellurium-doped InSb.

OBJECTIVES

The objectives of growing Te-doped InSb in Skylab were to confirm the advantages of zero-gravity environment, to obtain basic data on solidification, and to explore the feasibility of electronic materials processing in outer space. Thus, the experiment was designed to achieve diffusion-controlled, steady-state solidification and to investigate the associated growth segregation behavior on a micro- and macro-scale. Direct comparison of growth and segregation on earth and in space was to be achieved by melting and resolidifying in space a portion of each crystal grown on earth.

EXPERIMENTAL APPROACH

Crystal Growth Apparatus

The InSb growth experiment was carried out in the "multipurpose furnace" (Fig. 1) designed and constructed by Westinghouse Electric Corporation. The furnace provides for three tubular cavities into which three stainless steel cartridges containing the crystal growth assemblies are inserted. Heat levelers, lateral heat-shields, and the heat extractor plate insure controlled heat flow from the heating element to the heat extractor plate through the crystal. Melting is initiated at the end of the crystal (to be referred to as hot end), located inside the heating element and the crystal-melt interface is advanced to the desired position (back-melting) by appropriate power input. Regrowth, in turn, is achieved by controlled power reduction.

From heat transfer calculations and ground-based growth experiments, it was concluded that, in Skylab, a power input of 99 watts to the furnace containing three encapsulated InSb crystals should result in a melt zone approximately 6 cm long, with an initial thermal gradient of about 46°C/cm.

In ground-based tests it was found that the morphology of the crystal-melt interface was slightly concave (viewed from the melt). No prediction could be made, however, about the growth interface morphology under zero gravity conditions since the wetting characteristics of InSb melts and the associated radial heat transfer behavior was not known.

Crystal Preparation and Assembly

Indium antimonide used for ground-based tests and the Skylab experiment was synthesized in the Electronic Materials Laboratory at M.I.T. The single crystals for the experiment were pulled from the melt in the <111> direction by the Czochralski technique. The as-grown crystals (approximately 1.8 cm in diameter and 17 cm long) were centerless ground to a diameter of 1.4 cm, and cut to a length of 11 cm. The cylindrical crystals were etched in modified CP-4 (3 parts HF + 5 HNO_3 + 3 CH_3COOH + 10 H_2O) to remove surface damage and reduce their diameter to the desired value. Each crystal was subsequently inserted between graphite spacers into a quartz ampoule of 3 mm wall thickness. The diameter of every crystal was 0.13 mm smaller than the inside diameter of its ampoule.

The spacer at the hot end had a peripheral cylindrical cavity to provide additional space for the melt in case unforeseen surface tension effects under zero gravity conditions resulted in increased clearance between the regrown crystal and the quartz wall; the cylindrical graphite spacer at the other end of the crystal (to be referred to as cold end) was designed to enhance heat transfer from the crystal to the heat extractor plate. The crystals were positioned in the ampoules so that their B <111> direction coincided with the regrowth direction.

All ampoules were repeatedly flushed with purified helium and evacuated to 10^{-7} torr prior to sealing. The crystals were anchored near their cold end to the ampoules by means of a small depression in the quartz wall formed by local heating of the evacuated ampoules.

Each sealed ampoule was encapsulated by the Westinghouse Electric Corporation in an evacuated stainless steel cartridge and subjected to simulated launch and re-entry conditions; they were subsequently examined by radiography. One set of three cartridges containing an undoped crystal, a Te-doped crystal ($\sim 10^{18}/cm^3$) and a heavily Sn-doped crystal ($\sim 10^{20}/cm^3$) was selected for the zero gravity growth experiment (Skylab-III mission). A second set was selected for back-up purposes and was eventually used in an unscheduled second experiment in space (Skylab-IV mission). A sealed ampoule and its metal cartridge used in the Skylab experiment are shown in Fig. 2.

Crystal Growth Procedure in Space

Skylab-III Mission Experiment: The samples were inserted into the multipurpose furnace and back-melting was initiated by turning on the power. The desired back-melting was achieved in 120 minutes. Then the system was kept at temperature for a period of 60 minutes (soaking period), to achieve thermal equilibrium in the system and homogenization of the melts.* Subsequently, a cooling rate of 1.17°C/min was established by controlled power reduction at intervals of 14.4 sec. Four hours after initiation of regrowth the power was turned off and passive cooling to the ambient temperature took place. The thermal history of the growth system (hot end temperature) obtained from a chromel/alumel thermocouple in the furnace is shown in Fig. 3.

*A soaking period of 180 minutes was originally specified for this purpose; however, an inadvertent power shortage necessitated the reduction of the soaking period to 60 minutes.

Skylab-IV Mission Experiment: The remelting and thermal soaking procedure was identical with that of the Skylab-III experiment. However, in this (originally scheduled) experiment the growth system was subjected to a mechanical shock by striking the furnace assembly at a predetermined time; furthermore, the constant cooling rate of 1.17°C/min was interrupted 140 minutes after initiation of regrowth and a second thermal soaking period of 60 minutes was introduced by maintaining the furnace power at a constant level. The power was subsequently turned off and the system was allowed to reach ambient temperature (see Fig. 3). These changes in the growth procedure were intended to provide time reference markings in the crystal and to obtain data on the dependence of transient segregation on growth rate.

RESULTS AND DISCUSSION

The extent of regrowth achieved during the Skylab experiment was virtually the same for all crystals (about 6 cm) and in excellent agreement with theoretical calculations and ground-based testing; in each crystal the regrowth interface was clearly delineated (see for example Fig. 2).

Before proceeding with the analysis of the Te-doped crystals, it is of interest to discuss briefly the morphological characteristics of the Sn-doped and undoped crystals. The space-grown segments of the two Sn-doped crystals are shown in Fig. 4; the regrowth interface is clearly seen on the left-hand side of the figure. In both instances (as in the case of undoped InSb) the crystal surfaces, viewed through the quartz ampoule, are smooth and highly reflective, indicating that they formed in intimate contact with the confining walls. The presence of randomly distributed cavities of varying size, attributed to entrapped gas, indicates that the melt was also in intimate contact with (wetted) the quartz walls. The morphological characteristics

of the two crystals are identical; differences in phase (Sn) segregation are associated with differences in growth conditions.

MORPHOLOGICAL CHARACTERISTICS

All crystals were separated from their containers, without affecting their morphological characteristics, by dissolving the quartz ampoules in 48% HF.

The two Te-doped InSb crystals will be discussed individually since they exhibit seemingly significant differences in morphological characteristics.

Tellurium-Doped InSb Grown in Skylab-III

This crystal was of the same diameter as the earth-growth segment (seed), two portions of which are shown in Figures 5 and 6; they correspond to the early and late stages of growth, respectively. The surface of the crystal, in contrast to that of the Sn-doped and undoped crystals, has a dull appearance which indicates that during growth it did not establish contact with the confining quartz wall. This conclusion is reinforced by the absence of peripheral cavities which generally characterize growth under confined geometry.

The surface of the regrown crystal in the vicinity of the seed (Fig. 5) exhibits several bands of differing width oriented normal to the growth direction. These bands were identified as the external boundaries of rotational twins (see below) which are frequently encountered in InSb grown in the <111> direction.

Conspicuous in Fig. 6 is the presence of irregularly spaced "surface ridges" oriented preferentially in the direction of growth (left to right). The ridges are shiny at the top indicating contact with the quartz wall; they are, on average, 25 μm high and increase in width towards the hot end of the crystal. Over the last 10 mm of the crystal the ridges become irregular and

branch out. The regions between the ridges exhibit, in general, the characteristics of growth from free (unconfined) melts. In some isolated areas inclined lines, which have the appearance of stress-induced defects, originate at the surface ridges. These defects were shown to be confined to the surface region and to have no detectable effects on the growth and segregation behavior of the system. To the authors' knowledge, the phenomenon of surface ridge formation has not been previously observed in solidification under confined geometry; it will be further discussed below.

Tellurium-Doped InSb Grown in Skylab-IV

As seen in Fig. 7, regrowth, following the thermal soaking period, proceeds (top to bottom) first with decreasing and then essentially constant crystal diameter. With continuing growth the crystal diameter decreases, again, then increases and assumes a constant value of 12.8 mm (bottom of Fig. 7) which is the same as that of the T.D. of the confining quartz ampoule. (The reasons for the differences in diameter between the two Te-doped crystals in the early stages of regrowth will be discussed below.)

From volume considerations, it is concluded that the increase of the crystal diameter, with continuing growth coincides in time with the initial contact of the melt with the graphite spacer at the end of the quartz ampoule. Since crystal growth over the first 30 mm proceeded with a decreased diameter, and solidification of InSb is accompanied by a volume expansion of 12.9%, the volume available to the residual melt is less than during the Skylab-III experiment at the same time in growth. Thus, towards the final stages of solidification some melt was ultimately forced into the peripheral cavity available in the hot-end graphite spacer. Indium antimonide solidified in the spacer cavity weighed 2.52g. Accordingly, the total available volume for the melt in the ampoule itself (excluding the volume of the cavity in the

graphite spacer) was occupied after the crystal had reached a length of 34 mm, i.e., 5 mm after the crystal diameter reached its maximum value. Since the clearance between the spacer and the quartz wall was less than 0.25 mm, the melt was under substantially increased pressure during the last 25 mm of growth. This increased pressure, however, did not lead to forced wetting between the melt and the quartz wall since contact between the crystal and the wall remained confined to the surface of the irregularly spaced ridges as in the Skylab-III crystal.

The surface characteristics of the crystal grown with a diameter smaller than the I.D. of the ampoule are typical of free-surface solidification. They are identical with those encountered between the surface ridges in the Skylab-III crystal and are similar to those observed on crystals grown by the Czochralski technique on earth.

Figure 8 shows the surface characteristics of the crystal portion grown with constant reduced diameter at a distance of about 10 mm from the initial regrowth interface; the surface irregularities are the same as those commonly observed in non-faceted crystal growth from the melt. In addition, randomly spaced lines oriented normal to the <111> growth direction are visible. These lines are not continuous over the whole periphery and are confined to the three relatively flat portions of the crystal surface. They are not present on the centrally located "white" band which was identified as a rotational twin (see also below).

It is of interest to note that the crystal portion with a reduced diameter does not exhibit surface ridges observed on the previously discussed crystal. Surface ridges do, however, appear as the crystal diameter increases and approaches the value of the I.D. of the ampoule. Details of surface ridge

patterns are shown in Fig. 9. The ridges in this crystal are of the same height as those on the crystal grown in Skylab-III (~25 μm); here again they have no measurable effect on growth and segregation in the bulk of the crystal. They appear, however, less oriented along the growth direction and more branched. From the propagation patterns of these ridges, it is concluded that they are not the result of anomalous solidification, but, rather, that they are formed on the melt prior to solidification.

So far all attempts to account for ridge formation on the basis of known phenomena, such as wetting and convection induced by surface tension gradients, have met with fundamental inconsistencies.

Bulk Characterization

The bulk characterization of the space-grown crystals was aimed primarily at the growth and segregation behavior employing various analytical techniques. For this purpose the crystals were sectioned as shown in Fig. 10.

Dopant Segregation

The analysis of dopant segregation by high resolution differential etching was carried out on longitudinal sections of (211) surface orientation (see Fig. 10). All crystal sections were polished with Syton and etched for 40 seconds in a solution of 1 HF(48%) and 1 CH_3COOH (glacial) + 1 $KMnO_4$ (saturated aqueous solution); they were subsequently rinsed, dried in purified nitrogen and studied by means of interference contrast microscopy.

The striking difference in dopant segregation during growth under the influence of gravity and under zero gravity conditions is evident in Fig. 11 where a portion of earth-grown (upper part) and space-grown crystal (lower part) is shown. Compositional inhomogeneities which characterize the earth-grown segment (including pronounced coring effect) are absent in the segment grown in space. It is further seen that the regrowth interface morphology,

established during thermal soaking, is concave (viewed from the melt).

The sharp demarcation line separating the earth- and space-grown segment is the result of an abrupt decrease in Te concentration which is dictated, for initial regrowth, by the thermodynamic characteristics of the system, i.e., the distribution coefficient, k_o of Te in InSb is less than one ($k_o = C_S/C_L < 1$, where C_S and C_L are the concentration of Te in the solid and the melt, respectively).

The microscopic segregation behavior for the peripheral part of the crystal in the vicinity of the regrowth interface (right-hand side of Fig. 11) is shown in Fig. 12. Pronounced segregation fluctuations (compositional inhomogeneities) in the earth-grown segment reflect irregular variations in growth conditions which are due to rotation effects and to uncontrolled gravity-induced thermal convection in the melt. No microscopic compositional fluctuations are present in the crystal segment grown in space. In the central part of the crysta also (Fig. 13) irregular microsegregation variations are present in the earth-grown segment but not in the corresponding space-grown segment. The segregation behavior in the equivalent region of the crystal grown during the Skylab-III mission was identical to the behavior presented above.

According to theory, the area of the space-grown region shown in Fig. 13 must be part of a transition region over which the dopant concentration increases continuously until it reaches the same value as that of the dopant concentration present in the bulk of the melt; at this point steady-state segregation conditions are established and the dopant concentration in the solid remains constant except at the very terminal stage of solidification.

Quantitative Dopant Segregation Analysis

Since one of the major objectives of the Skylab experiment was to achieve

steady-state segregation, quantitative dopant concentration analysis of the transition region was undertaken by means of Hall-effect measurements and ion-microprobe scanning.

Hall-effect measurements were carried out by the Van der Pauw technique in a 6" field-regulated electro-magnet employing a constant current source and a calibrated, high impedance micro-volt detector. The Hall-effect samples were squares 2 mm x 2 mm and 0.5 mm thick. Quadrant-shaped silver contacts were evaporated at the four corners of each sample and were annealed at 350°C for two hours to ensure ohmic behavior. Subsequently, gold wire leads were soldered with indium onto the contacts (Fig. 14). More than thirty individual Hall-effect measurements (at different field strengths) were carried out on each sample to optimize the validity of the data. The reproducibility of the results was better than one per cent.

Hall-effect measurements were carried out on the Te-doped crystal grown in the Skylab-III mission. Twelve successive crystal slices, 0.5 mm thick, were cut, as shown in Fig. 10. Two adjacent Hall-effect samples (2 mm x 2 mm) were chosen from each slice, in most instances near the central part of its straight edge (corresponding to a central location in the crystal). For some slices the Hall-effect samples could not be taken from the central location since twin or grain boundaries were present.

The compositional (carrier) profile together with the corresponding resistivity and carrier mobility obtained at 77°K are shown in Fig. 15. Hall-effect measurements on all samples were also performed at room temperature. The room temperature data are not significantly different than those shown in Fig. 15 in view of the relatively high level of carrier concentration.

The carrier concentration curve (N_{space}) in Fig. 15 shows clearly the decreased dopant concentration in the initial part of the space growth region,

as predicted from theory; it delineates further the transient region in which the dopant concentration increases steadily and reaches its maximum value at a distance of about 0.5 cm from the regrowth interface. Beyond this distance the dopant concentration remains constant for the entire crystal length analyzed (5 cm); it is, thus, shown that ideal steady state segregation and homogeneous dopant distribution was achieved under zero gravity conditions. Ideal steady state segregation has never been achieved on earth. In the ground-based tests performed in an identical experimental configuration and under "stabilizing thermal gradients" as seen in Fig. 15, the dopant profile for the ground-based experiment (N_{earth}) indicates clearly a steadily increasing dopant concentration which reflects the presence of convective interference apparently due to convection caused by unavoidable lateral thermal gradients.

The ratio of the dopant concentration in the initially grown region and in the steady state-grown region is a direct measure of the equilibrium distribution coefficient, k_o, which cannot be reliably determined on earth. Unfortunately, the low spatial resolution of Hall-effect measurements does not permit, at this time, the accurate determination of k_o. From the width of the region of transient segregation and the associated compositional change, the diffusion coefficient of the dopant in the melt can be determined, provided the microscopic growth rate is known and constant; this condition was not met in the present experiment, since only the nominal growth rate is known.

It should be pointed out that the observed variation in carrier concentration between adjacent Hall samples is not surprising since extensive twinning took place in this InSb crystal in view of the fact that its diameter was the same as that of the confining wall and solidification is accompanied by 12.9 per cent volume expansion. In addition to twinning, growth under these

conditions leads to high dislocation densities which account for the measured relatively low, carrier mobilities. In contrast, in the crystal grown during the Skylab-IV mission, with a smaller diameter than that of the quartz ampoule (unconfined solidification) the dislocation density was found to be 40 per cent smaller than that in the earth-grown segment.

The compositional profile in the same crystal was in parallel investigated by means of an ion microprobe analysis since this technique was expected to provide a similar sensitivity as the Hall-effect measurements but a resolution in the micron range. Measurements carried out with a CAMECA, IMS 300 Ion Analyzer and with an Applied Research Laboratory, Ion Microprobe Mass Analyzer are essentially consistent with the results of the Hall-effect measurements; however, due to the relatively low yield of sputtered Te-ions, the linear resolution and accuracy were found to be limited. Thus, as seen in Fig. 16, the precision of the ion-microprobe results with a scanning beam of 25 μm was only of the order of $\pm$16%.

Intentionally Introduced Segregation Discontinuities

As pointed out earlier, the growth process during the Skylab-IV mission was perturbed 90 minutes and 140 minutes after initiation of the cooling cycle by a mechanical shock and by an arrest of cooling, respectively; the cooling arrest was sustained for a period of 60 minutes. These perturbations were intended to introduce time reference markers in the crystal and to study their specific effect on segregation behavior under steady state conditions.

Etching analysis of the crystal revealed the presence of only two distinct segregation discontinuities manifested as curved lines, extending over the entire cross-section of the crystal, 15 mm and 28.8 mm from the initial regrowth interface. As seen from the sketch in Fig. 17, the first discontinuity

coincides with an abrupt decrease in crystal diameter and is of relatively low intensity as viewed in interference contrast. The second discontinuity was formed after the crystal had reached its maximum constant diameter and is very pronounced as seen in Fig. 18.

The nature of these segregation discontinuities was investigated by double beam interferometry. As seen in Fig. 19a, the first perturbation (15 mm from the initial regrowth interface) resulted in a small and localized increase in tellurium concentration; on the other hand, the second perturbation (Fig. 19b) resulted in a pronounced segregation discontinuity (decrease) which persisted for an extended period of time. Thus, this second discontinuity is unambiguously identified as a transient segregation region associated with regrowth following thermal soaking. Accordingly, the first, short-lived, segregation discontinuity is associated with the mechanical shock.

Identification of the two segregation discontinuities permits their use as time markers for the determination of average microscopic growth rates in two different portions of the crystal. Thus, the average growth rate from the initial regrowth interface to the first discontinuity, 90 minutes into growth, is found to be 2.8 μm/sec and the growth rate from the first to the second discontinuity is 4.6 μm/sec. The average growth rate over the first 2.88 cm of growth (see Fig. 17) is 3.4 μm/sec.

The above growth behavior is consistent with theory: for the thermal configuration in the multipurpose furnace the thermal gradient in the melt is expected to decrease with continuing solidification and consequently the growth rate must correspondingly increase.

It is of interest to note that the fringe deflection at the second compositional discontinuity (Fig. 19b) is constant over the entire crystal

diameter. Since the fringe deflection is proportional to the concentration change across the discontinuity and since the dopant concentration in the initial regrowth portion at the discontinuity (following thermal soaking) must be constant across the crystal diameter, it must be concluded that the tellurium concentration in the crystal above the discontinuity, which is constant along the growth axis, (fringes parallel to the growth axis) must also be constant in the radial direction.

Crystal Morphology

As discussed earlier, the surface morphological characteristics of both space-grown crystals indicate that the Te-doped InSb melt does not wet the confining quartz wall. Accordingly, the contact angle between the seed and the melt at the peripheral contact line is controlled by the interfacial tensions of the three phases involved and the meniscus of the melt (which determines the shape of the growing crystal) becomes a function of the radius of curvature of the crystal-melt interface. The decrease in crystal diameter observed during the early stages of growth in the Skylab-IV experiment (Fig. 7) is, thus, a direct consequence of the pronounced concave configuration of the crystal-melt interface (as viewed from the melt) brought about by the thermal characteristics of the system.

The ensuing gradual change to constant crystal diameter reflects the decrease in lateral heat-transfer (due to the increasing distance of the growing crystal from the quartz wall) which results in an increase of the radius of curvature of the regrowth interface. The second decrease in crystal diameter, which coincides with the intentional, mechanical-shock perturbation, is attributed to a deformation of the melt (stretching towards the hot end) which established a melt menicus leading to decreasing crystal

diameter. The subsequent increase in the diameter of the crystal is due to the fact that the volume available to the growth system becomes limited.

In the Skylab-III experiment the radius of curvature of the initial growth interface was significantly larger than in the Skylab-IV experiment; accordingly, the crystal diameter in the Skylab-III experiment conformed to the size of the confining quartz wall.

Peripheral Facet Effect

Basic thermodynamic parameters are responsible for the fact that during growth of InSb in the <111> direction a facet is generally formed at the growth interface. Since facet formation is associated with kinetic supercooling, the facet is centrally located at convex interfaces and peripherally at concave interfaces (as viewed from the melt). It is generally believed that dopant segregation within facets is controlled by lateral layer growth rate which is sensitive to thermal perturbations and gravity induced convection.

Consistent with the above considerations, peripheral facet formation is observed in both space-grown crystals (Fig. 20) since in both experiments the growth interface assumed concave morphology (Fig. 17). The well-defined segregation discontinuities on the facet grown region cannot, however, be explained on the basis of thermal and/or convective perturbations in the melt since segregation in the bulk of the crystals was found to be homogeneous.

The observed segregation effects in the peripheral facets can be explained by considering that kinetic supercooling for peripheral facet formation assumes its highest value at the outermost part of the growth interface, which thus becomes the location with the highest probability for nucleation of lateral layer growth. Under these conditions, any perturbation,

such as a vibration or the arrival of a foreign particle at the peripheral three-phase contact line may trigger spurious nucleation of lateral layer growth and, thus, result in the formation of the observed segregation discontinuities. Their magnitude (intensity) is seen to decrease with decreasing supercooling from the periphery to the interior. Furthermore, depending on their magnitude, the facet segregation discontinuities extend more or less into the adjacent off-facet region; accordingly, it must be concluded that a finite amount of kinetic supercooling is associated with growth adjacent to facet regions. There is some evidence that the randomly spaced lines visible on the surface of the grown crystal (Fig. 8) correspond to the external boundaries of the presently discussed facet segregation discontinuities.

It should be pointed out that the same type of facet segregation discontinuity has been observed superimposed on compositional inhomogeneities in facet regions of earth-grown InSb; their origin could not, however, be explained.

Rotational Twinning

The bands of varying width appearing on the left-hand side of the crystal grown during the Skylab-III experiment (Fig. 5) were identified as the external boundaries of $(\bar{2}11)$ rotational twins. Each band is the result of two consecutive rotations by 60° of the (111) plane normal to the growth direction.

Analysis of the rotational twins on etched crystal segments of (211) surface orientation (Fig. 21) shows that some propagate across the entire crystal, some terminate within the crystal, and others deteriorate to grain boundaries, eventually leading to breakdown of the single crystal matrix.

In view of the concave interface morphology, nucleation during growth is essentially restricted to the outermost peripheral part of the growth interface which, as discussed previously, is susceptible to spurious nucleation. Rotational twin formation initiated by a nucleus having a 60° misorientation within the growth plane can thus be explained as the result of spurious nucleation of the crystal periphery.

Because of inherent thermal asymmetry in the multi-purpose furnace, the concave growth interface morphology is to some extent inclined to the growth direction. Therefore, any misoriented nucleus formed at the lowest part of the three-phase contact line (periphery of the growth interface) encounters no constraints in propagating and results in the formation of a twin boundary which crosses the entire crystal. Spurious nucleation at any higher part of the periphery, however, can propagate only through part of the crystal, since a varying fraction of the plane of propagation has solidified already in the original orientation. Considering that a twin boundary cannot terminate within the crystal, its direction of propagation must change to form a curved grain boundary which may either terminate at a subsequently nucleated twin boundary or lead to a polycrystalline matrix (see Fig. 21). It is of interest to note that the tendency of twin formation is strikingly reduced (only one rotational twin was observed) in the crystal grown with reduced diameter during the Skylab-IV experiment.

CONCLUSIONS

The present InSb experiment proves unambiguously the uniqueness of zero-gravity conditions for obtaining directly fundamental data on crystal growth and segregation associated with solidification. Furthermore they

demonstrate the striking advantages of processing materials in space.

Specifically the following results and conclusions were obtained for the first time:

Ideal steady-state growth and segregation (exclusively diffusion controlled) were achieved leading to three-dimensional chemical homogeneity on a microscale over macro-scale dimensions (several centimeters in the present case); the transient segregation profile preceding steady state solidification was determined; limitations in the experimental arrangement and in the presently available microanalytical techniques do not permit, at this time, the extraction of fundamental data pertinent to solidification.

Surface tension effects led to phenomena previously never observed and theoretically not predicted: the Te-doped melt, not wetting the quartz wall, solidified with a free surface (unconfined) configuration. Under forced contact conditions, intimate contact between the melt and the confining walls was prevented, and the growth system was essentially isolated from its container by the formation of narrow surface ridges. It was also shown that surface tension effects in space remained localized on the surface and did not affect growth and segregation in the bulk.

In the absence of convective interference it was possible to identify segregation discontinuities associated with facet growth and to explain their origin on the basis of spurious nucleation. The absence of convective interference permitted, further, the determination of the mode of nucleation (formation of misoriented nuclei at the three-phase boundary line) and propagation of rotational twinning.

A mechanical-shock perturbation intentionally introduced during growth was identified in the crystal and found to cause a localized increase in

dopant segregation; this dopant discontinuity was used as a time reference for the determination of the average macroscopic growth rate.

On the basis of the present results it is no longer a matter of speculation that fundamental data necessary for bridging the gap between theory and experiment can be reliably obtained in the absence of gravity and that outer space presents one of the greatest opportunities ever afforded science and technology.

ACKNOWLEDGEMENTS

The authors wish to express their appreciation to the National Aeronautics and Space Administration, and particularly to the Staff at the Marshall Space Flight Center for their uncompromising efforts, cooperation and enthusiastic support during all stages of the experiment. They are indebted to Dr. K. M. Kim for carrying out much of the ground-based testing, to Drs. J. R. Carruthers and J. Colbey for stimulating discussions and to Mr. W. J. Fitzgerald and J. Baker for their skillful assistance with the characterization program. Finally, the authors are grateful to Dr. R. K. Lewis and the CAMECA Instruments, Inc., for their generosity in carrying out Ion-Microprobe Analyses of the crystal.

BIBLIOGRAPHY

The following bibliography is intended to provide pertinent background information.

J. C. Brice, "The Growth of Crystals from Liquids", North-Holland Publishing Co., 1973.

B. Chalmers, "The Principles of Solidification", J. Wiley, 1964.

J. J. Gilman, Editor, "The Art and Science of Growing Crystals", J. Wiley, 1963.

P. F. Kane and G. B. Larrabee, "Characterization of Semiconductor Materials", McGraw-Hill Book Company, 1970.

R. A. Laudise, "The Growth of Single Crystals", Prentice-Hall, 1970.

W. G. Pfann, "Zone Melting", 2nd ed., J. Wiley, 1966.

D. P. Woodruff, "The Solid-Liquid Interface", Cambridge University Press, 1973.

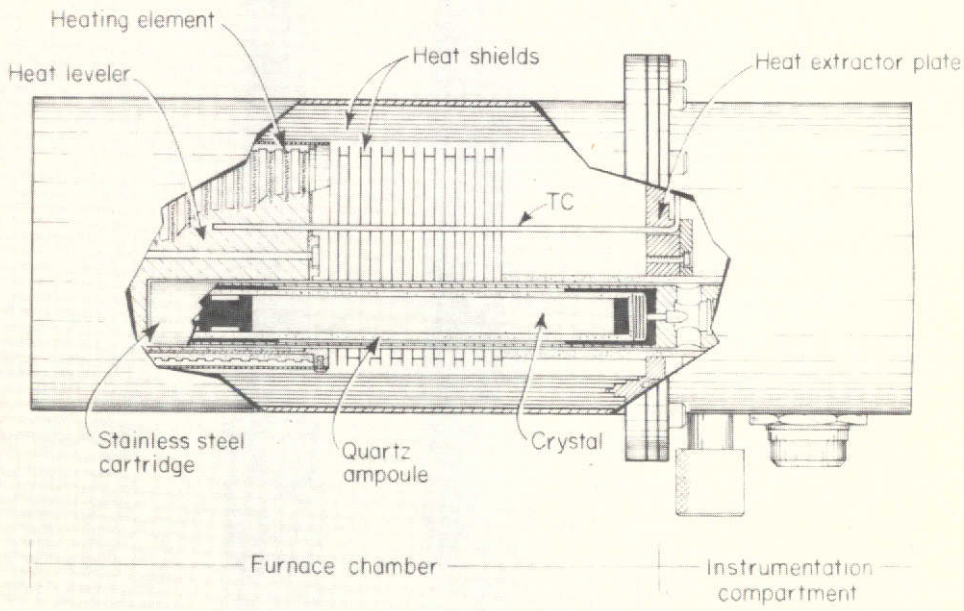

Figure 1 Sketch of the multipurpose furnace employed for the InSb growth experiment in Skylab.

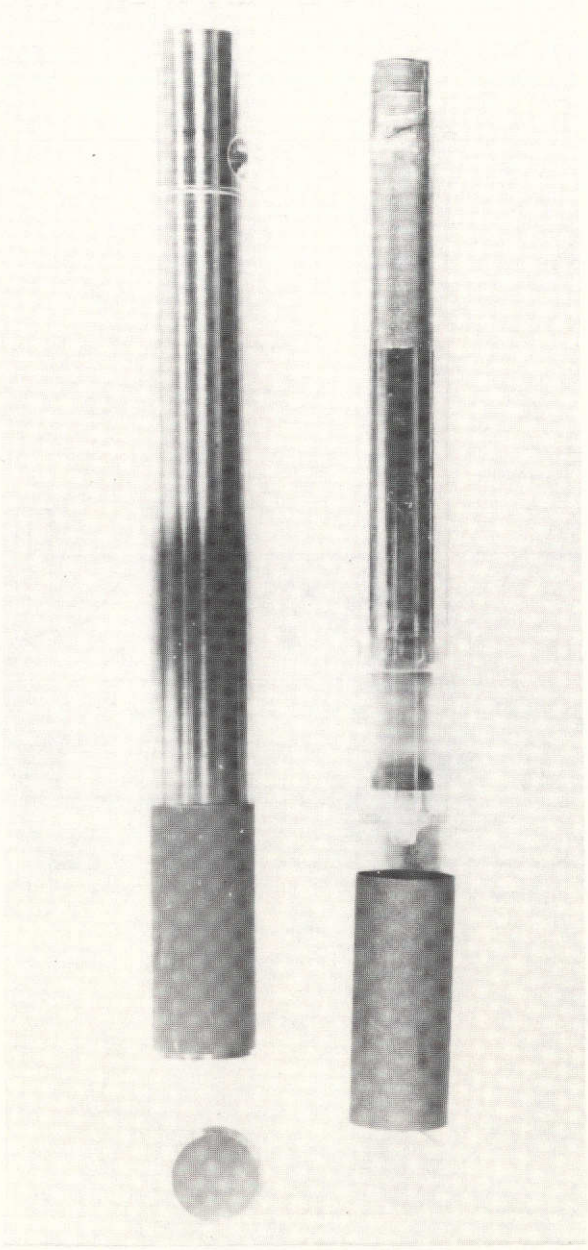

Figure 2 Right: Quartz ampoule containing InSb crystal used in the Skylab experiment; the cold-end graphite spacer, the earth-grown crystal segment, the space-grown segment and the hot-end graphite spacer with a peripheral cavity are seen from top to bottom; detached at bottom is the graphite sleeve positioned between ampoule and the metal cartridge. Left: Stainless steel cartridge in which ampoule was encapsulated.

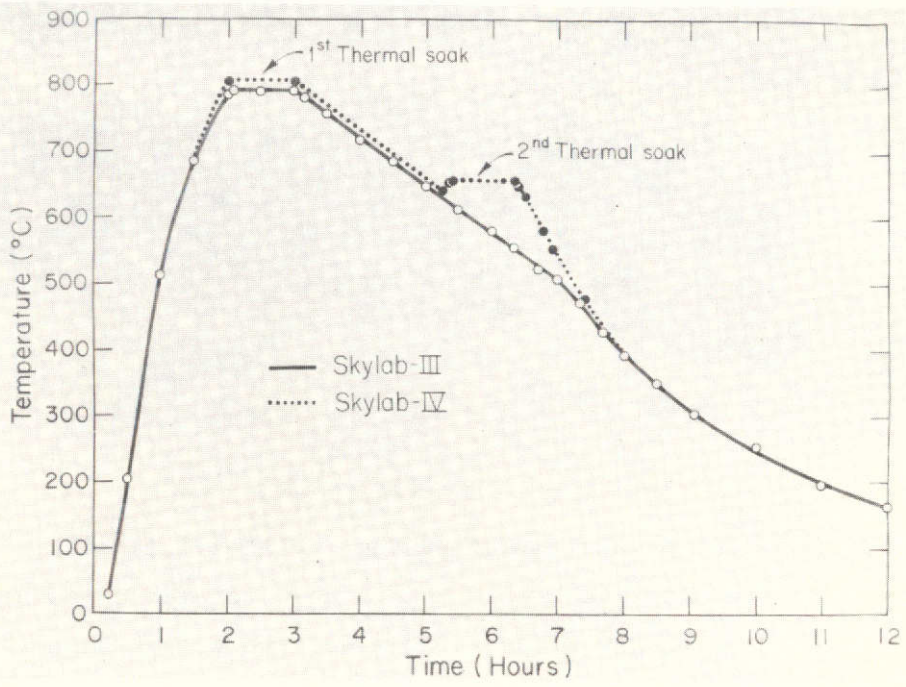

Figure 3 "Hot end" temperature cycles for Skylab-III and Skylab-IV experiments as obtained from a chromel/alumel thermocouple.

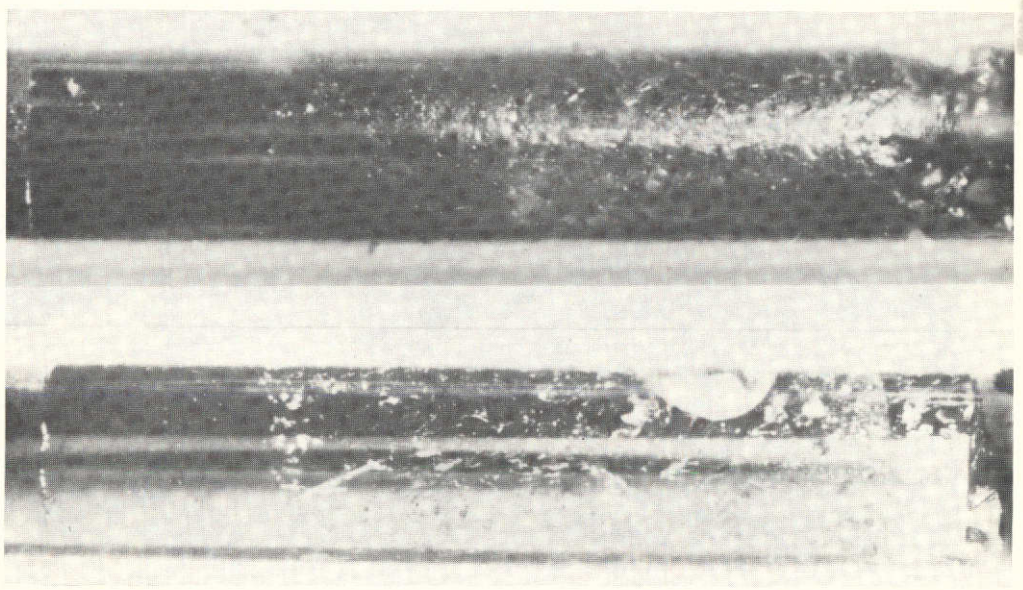

Figure 4 Heavily Sn-doped InSb crystal grown in space during Skylab-III (bottom) and Skylab-IV missions contained in the quartz ampoules. The initial regrowth interfaces are visible on the left-hand side of the figure; 2.6x.

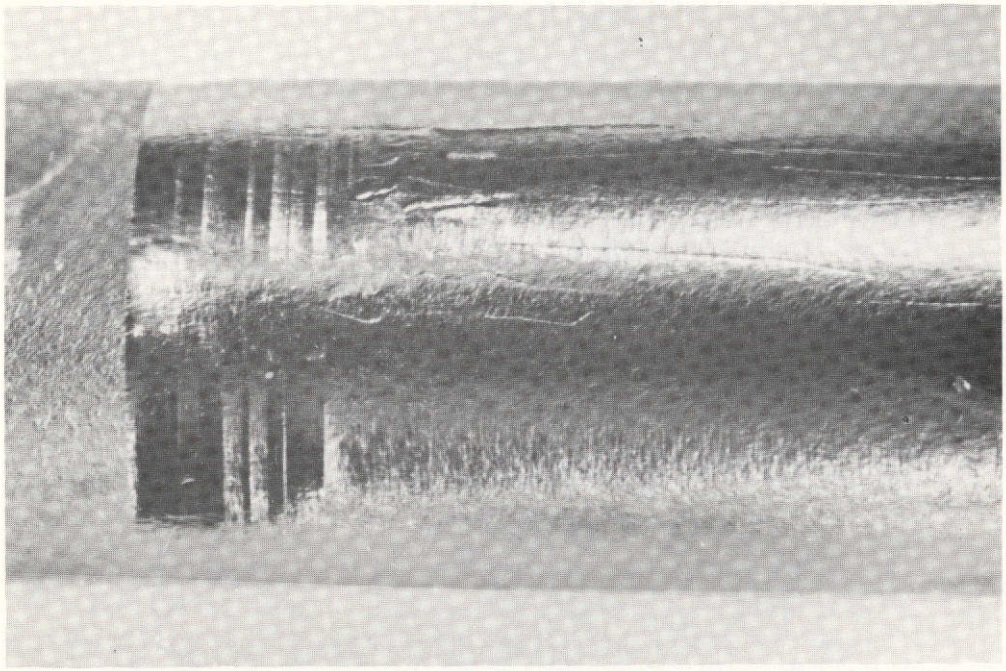

Figure 5 Te-doped crystal grown during Skylab-III mission. Note initial growth interface (left-hand side), rotational twin bands and surface ridges propagating along the growth direction; the diameter of the space-grown segment is the same as that of the earth-grown segment; 4.9x.

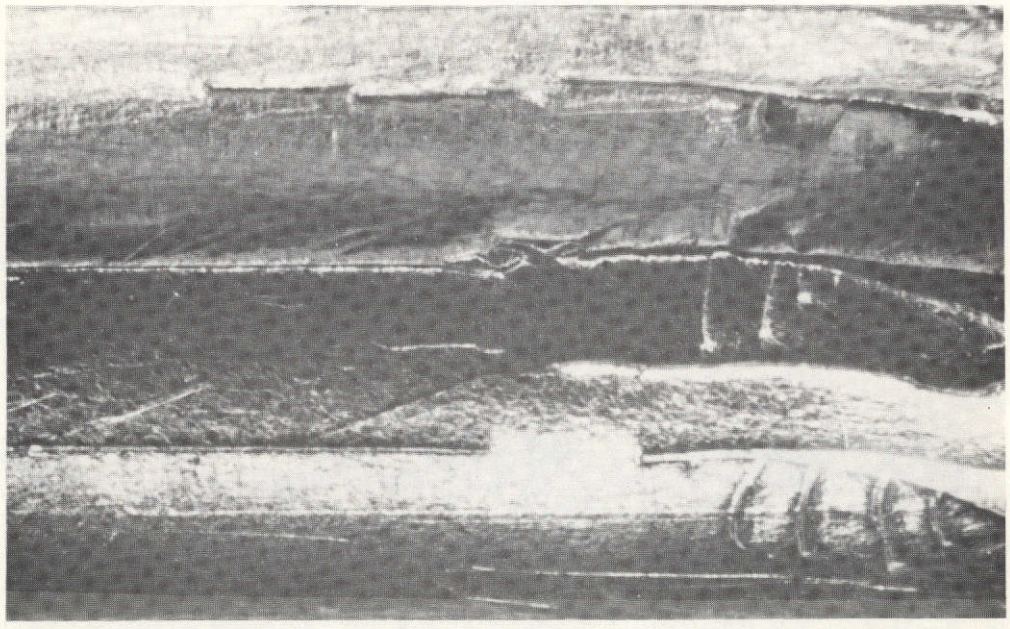

Figure 6 Part of the Te-doped crystal, grown during Skylab-III mission, 3.7 to 5.9 cm from the initial regrowth interface. Surface ridges broaden and branch out at the late stages of growth (right-hand side); 6.8x.

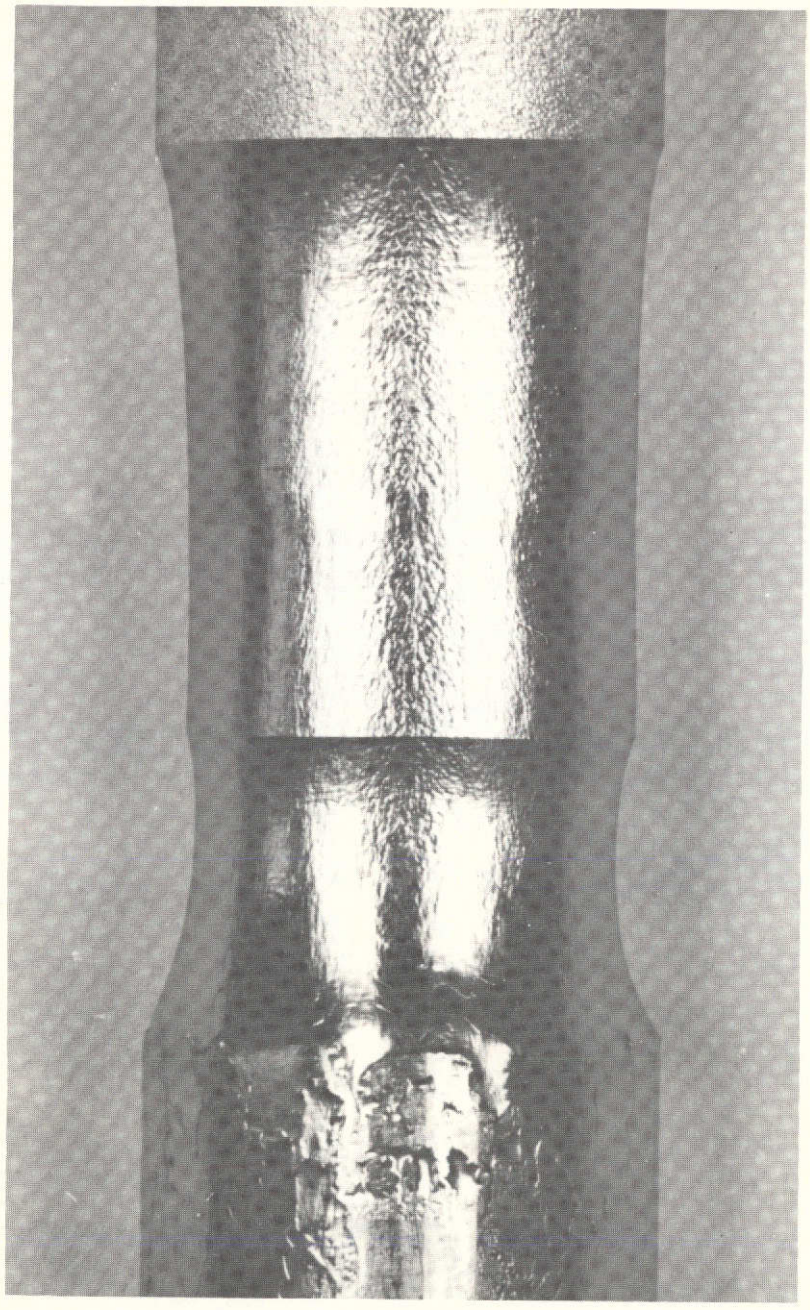

Figure 7 Te-doped crystal grown during the Skylab-IV mission; note decrease in crystal diameter upon initiation of growth; surface ridges appear towards the bottom after crystal diameter reaches its maximum constant value; 4.8x

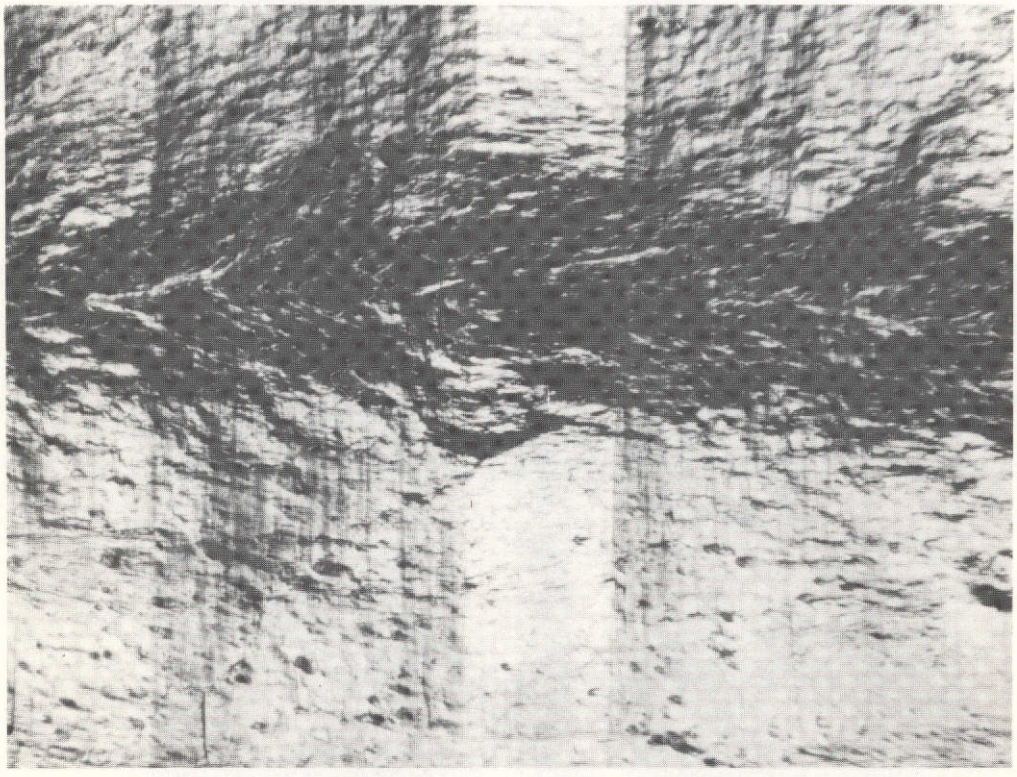

Figure 8 Part of Te-doped crystal shown in Fig. 7; surface characteristics are typical for unconfined solidification; note random distribution lines normal to the growth direction; rotational twin is visible (white band); 19x.

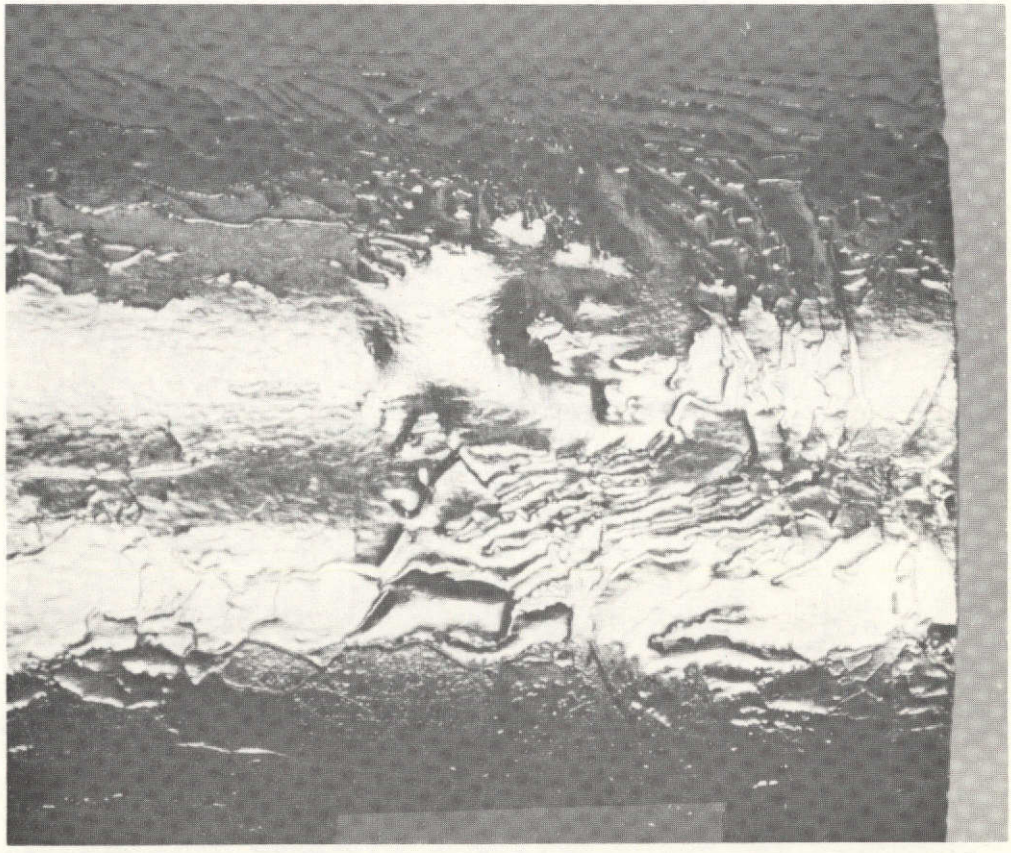

Figure 9 Surface ridge patterns formed after crystal reached maximum constant diameter during Skylab-IV experiment; note discontinuity in surface morphology associated with second thermal soaking (see text); 21x.

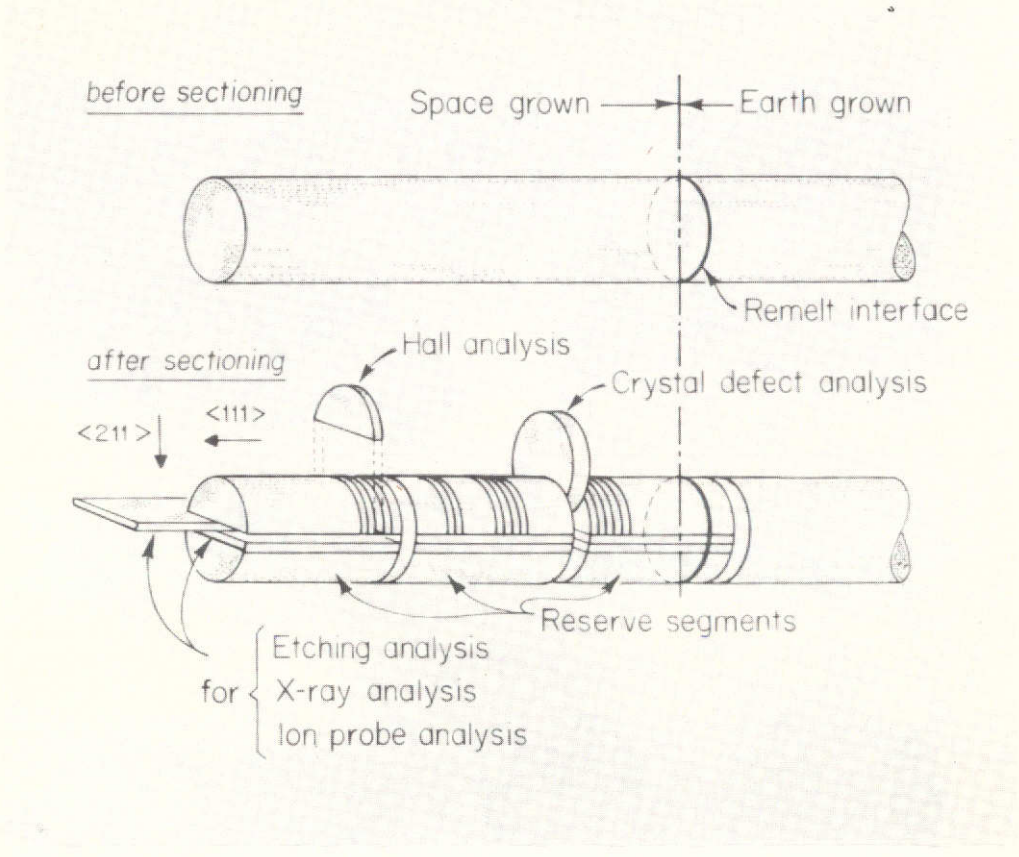

Figure 10 Sectioning scheme for analysis of space-grown crystal.

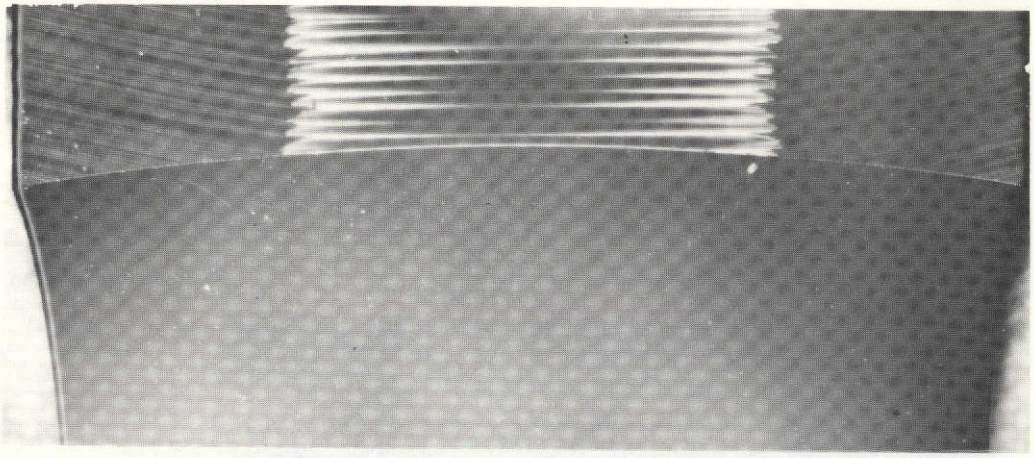

Figure 11 Etched cross-section (under dark field illumination) of crystal grown during Skylab-IV mission; space-grown region (bottom), in contrast to earth-grown region (top), exhibits no compositional inhomogeneities; 12x.

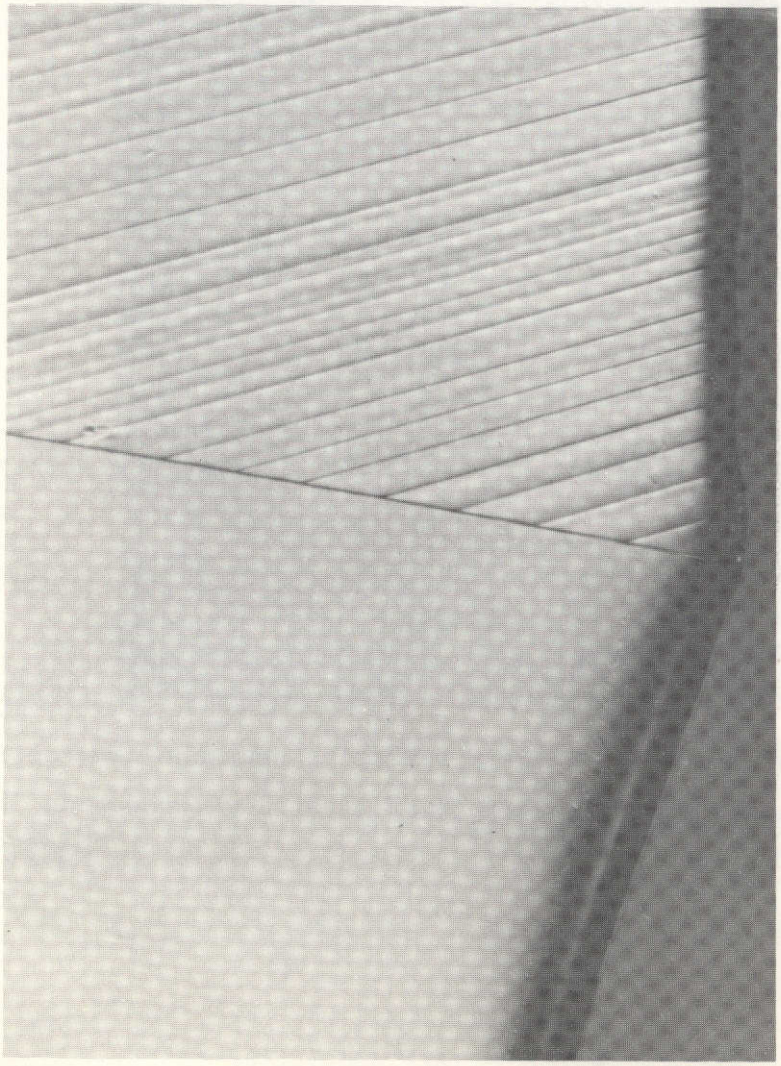

Figure 12 Dopant segregation characteristics near the periphery of initial regrowth interface (right-hand side of Fig. 11); 300x.

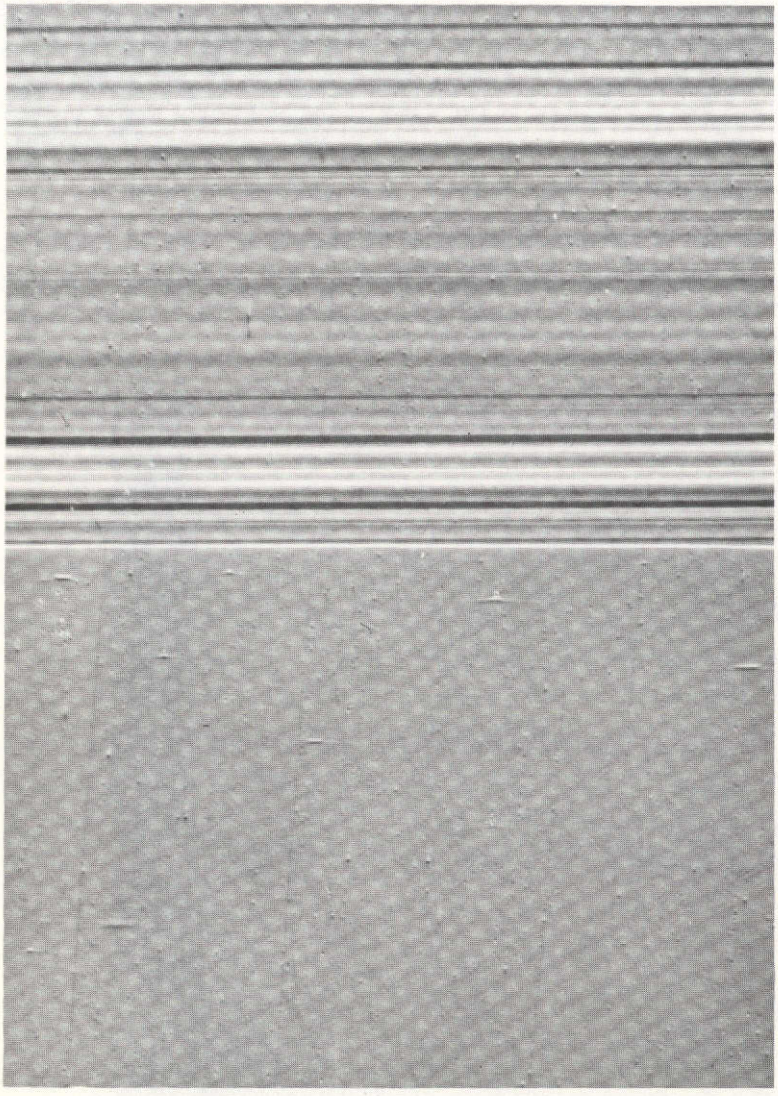

Figure 13 Dopant segregation characteristics near the central region of initial regrowth interface of crystal grown during Skylab-IV mission; 580x.

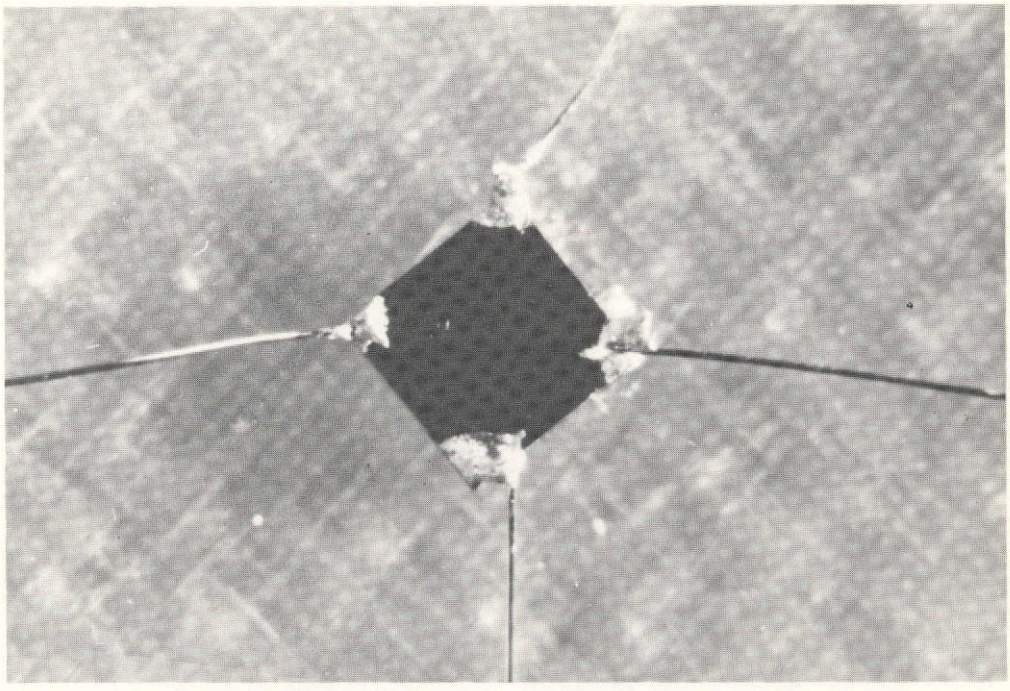

Figure 14 Sample for Hall-effect measurements (Van der Pauw configuration).

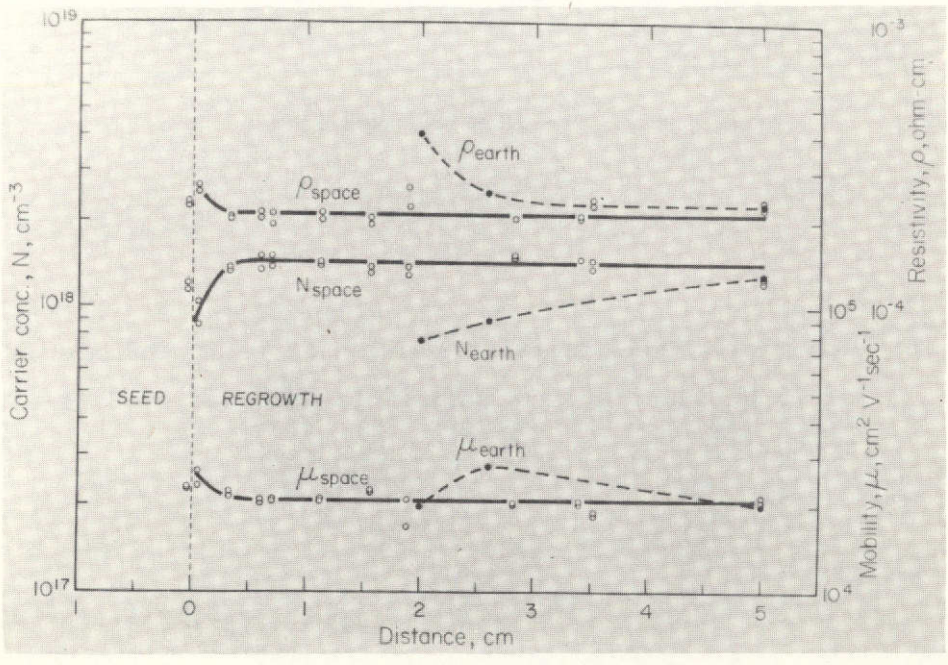

Figure 15 Carrier (dopant) concentration profile obtained from Hall-effect measurements for Te-doped crystal grown during Skylab-III mission (N_{space}) and for Te-doped crystal grown during ground-based testing (N_{earth}).

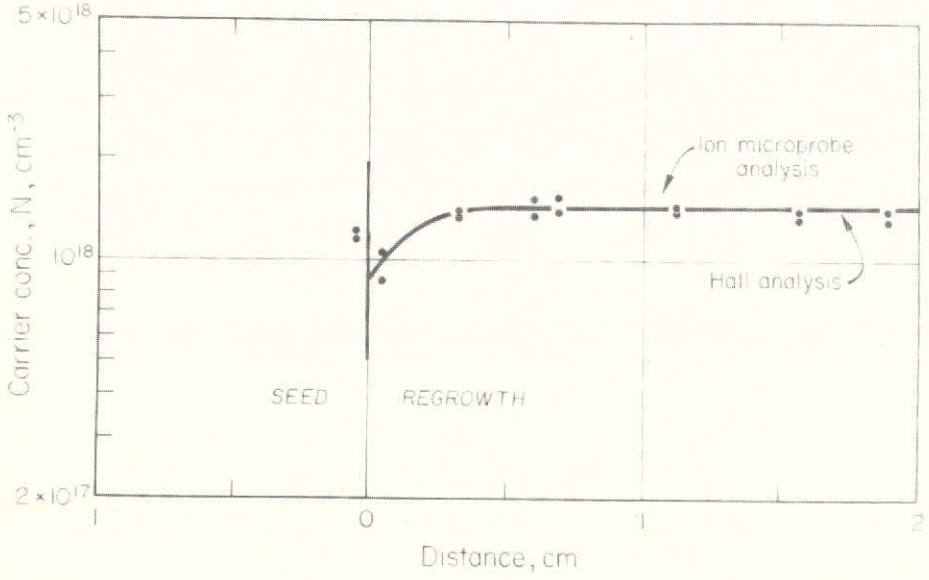

Figure 16 Ion-microprobe precision limits for Te in InSb for a beam size of 25 μm superimposed on profile obtained by Hall-effect measurements.

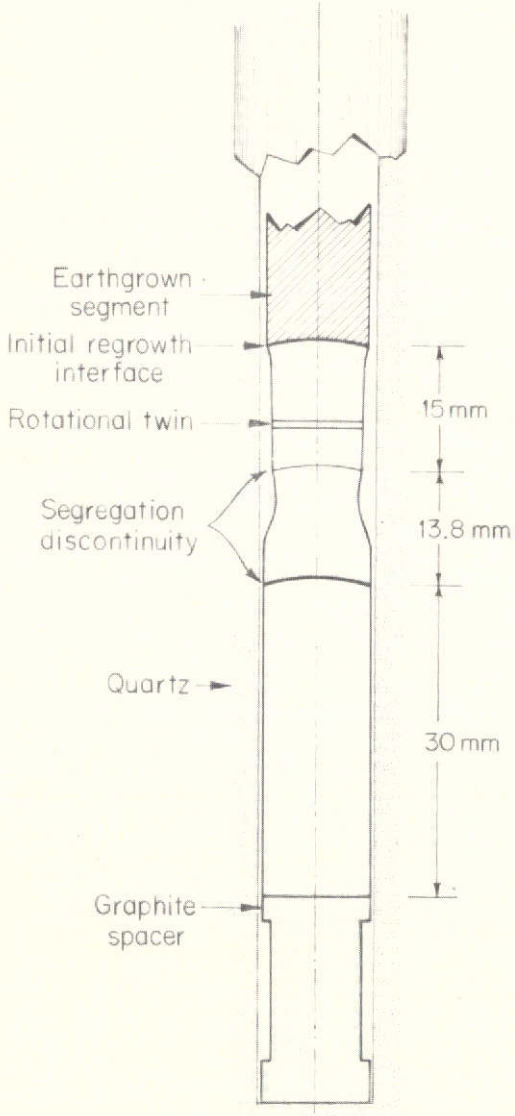

Figure 17 Cross-section of crystal grown during Skylab-IV mission.

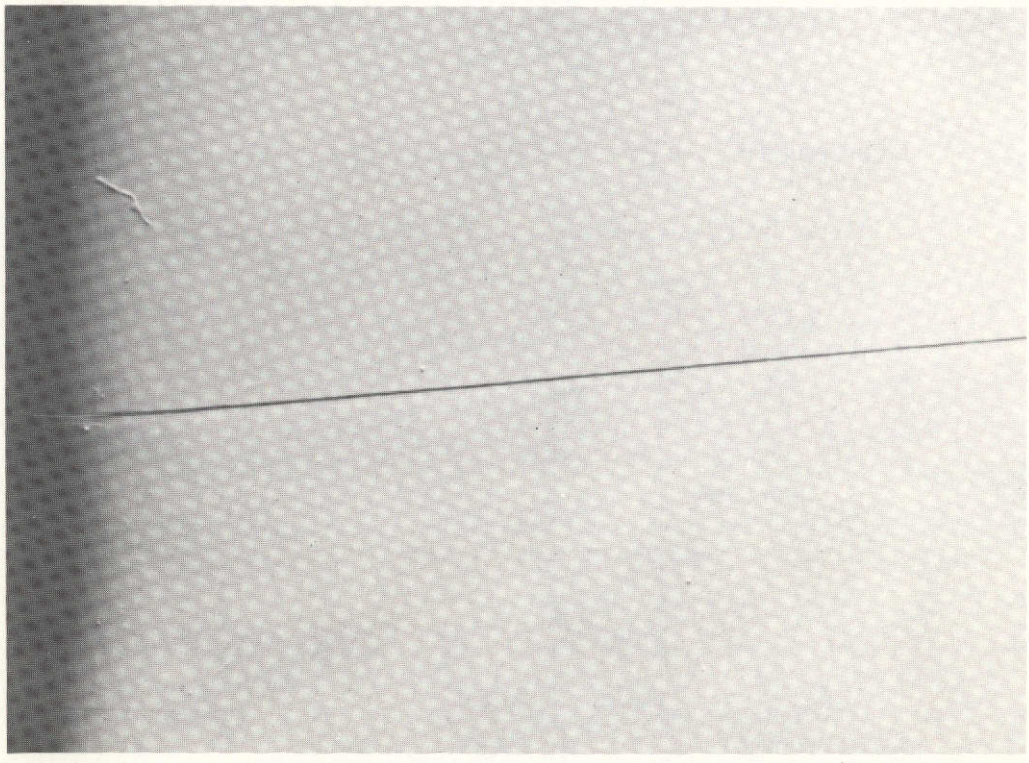

Figure 18 Dopant segregation discontinuity caused by cooling arrest and thermal soaking during growth in Skylab-IV mission; 400x.

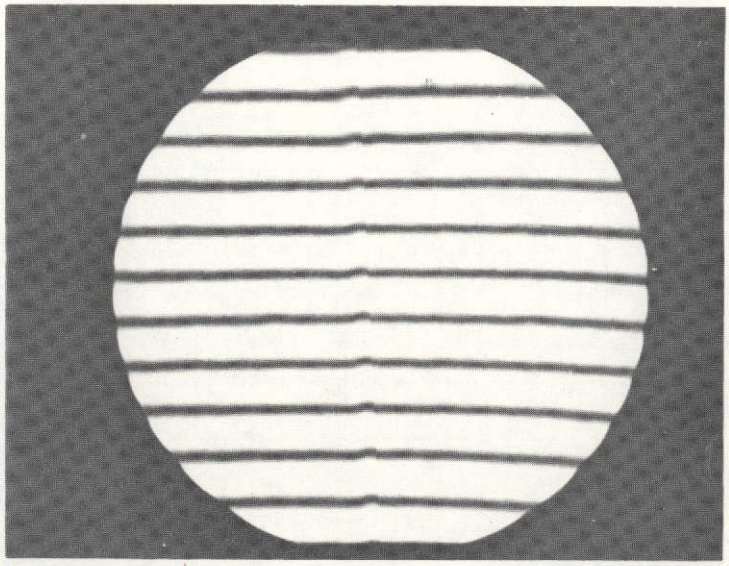

(a)

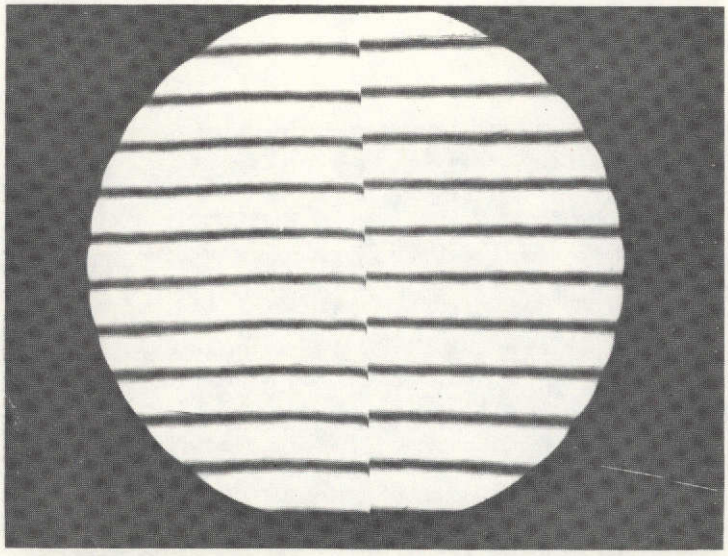

(b)

Figure 19 Double beam interferograms of segregation discontinuities as revealed by etching (a) caused by mechanical shock and (b) caused by regrowth after thermal soaking (see text).

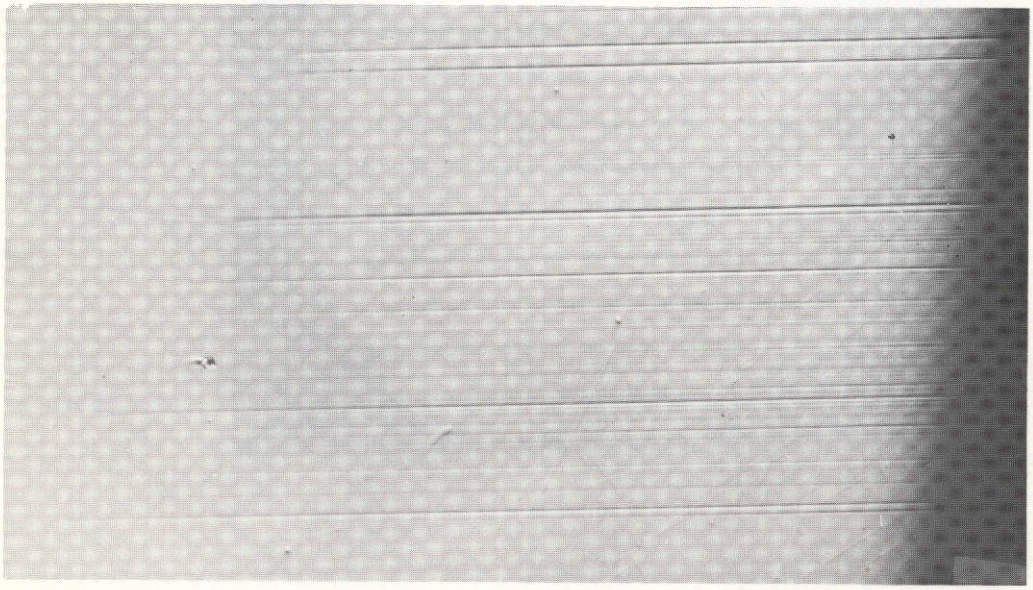

Figure 20 Peripheral facet growth with segregation discontinuities in crystal grown during Skylab-IV mission; 300x.

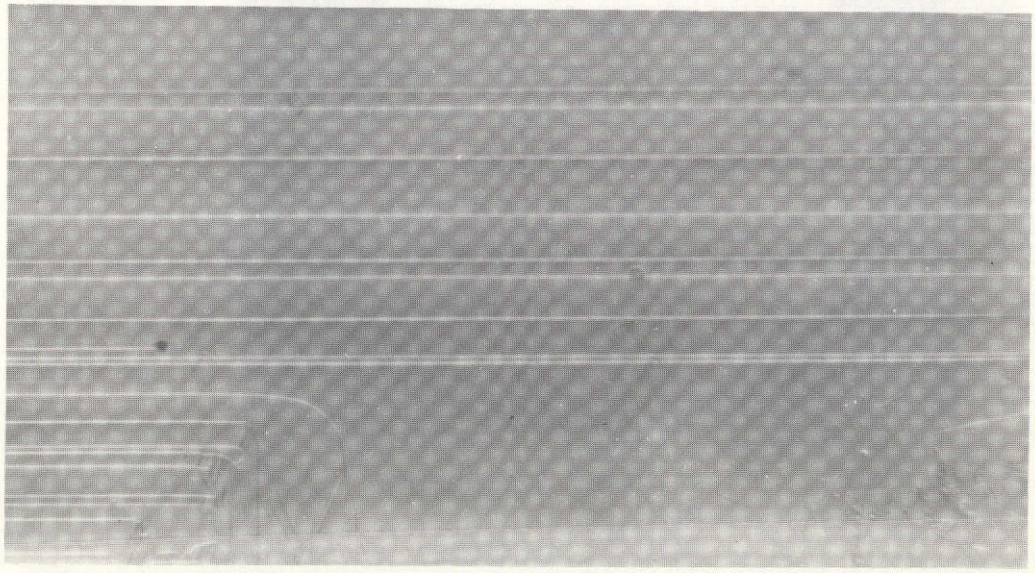

Figure 21 Cross-section of crystal grown during Skylab-III mission exhibiting rotational twinning (see also Fig. 5); 12x.

APPENDIX A

MATERIALS

Indium Antimonide:

The InSb used for ground-based tests and for all Skylab experiments was synthesized from the elements (In and Sb, both 99.9999% pure) at 600°C in a hydrogen atmosphere (800 mm Hg). After solidification the InSb was etched for three minutes in dilute CP-4 (5 parts conc. HNO_3 + 3 parts 48% HF + 3 parts glacial CH_3COOH + 7 parts H_2O) and used in ingots of 240 g for growth of the crystals required.

Dopant Elements and Doping Procedure:

The dopant elements (Te, 99.9999% in powder form and Sn 99.9999% in pellet form) were directly added to the solid InSb charge in the Czochralski crystal puller. The amounts of dopant required to achieve average doping levels of $\sim 10^{18}/cm^3$ (Te) and $\sim 10^{19}/cm^3$ (Sn) were calculated, taking the effective segregation coefficients as 0.8 and 0.05, respectively.

Graphite:

The graphite parts used were manufactured from A.T.J. grade graphite (National Carbon). All parts, after machining, were fired at 1000°C in vacuum (10 μm Hg) for two hours to remove volatile impurities. The following parts were made of graphite: crucibles used for ingot preparation and for single crystal growth (separate crucibles were employed for the growth of undoped, Te-doped and Sn-doped material); molds for the production of polycrystalline InSb test-samples used during the preliminary stages of ground-based experiments in the "SIM" and "prototype" furnaces; electrodes used for transmission of current pulses across the crystal-melt system to achieve growth interface demarcation during growth in the prototype multipurpose furnace; terminal spacers used in the quartz ampoules to facilitate heat transfer (cold-end

spacer) and to provide additional volume for the melt (hot-end spacer).

Quartz:

All ampoules used to encapsulate the crystals were made of G.E. 204-type quartz tubing with 3 mm wall thickness. All quartz parts used for encapsulation of the InSb crystals were etched with HF (48%), rinsed with distilled-de-ionized water and dried in a jet of purified nitrogen.

Preparation of InSb Crystals Used for Ground-Based Testing and Skylab Experiments:

A total of eighteen crystals were prepared and encapsulated into quartz ampoules in connection with the Skylab experiment; of these, three were polycrystalline samples used by Westinghouse for testing the prototype multi-purpose furnace. The polycrystalline samples (one each undoped, Te-doped and Sn-doped) were prepared in a modified Czochralski puller by melting the ingot material in a suspended graphite mold with the same I.D. as the quartz ampoules used for encapsulation. The graphite molds containing the molten InSb were lowered through the heat zone yielding polycrystalline ingots, solidified under stabilizing thermal gradients at a rate of about 10 μm/sec. The ingots were removed from the molds, cut to the appropriate length, etched in dilute CP-4 and encapsulated.

The single crystalline samples were grown in a Czochralski puller designed and constructed at M.I.T. All crystals were pulled under seed rotation (25 rpm) and counter crucible rotation (5 rpm). The pulling rates were 2"/hr for undoped 1.5"/h for Te-doped and 3/4"/h for Sn-doped material. All crystals (approximately 1.8 cm in diameter and 17 cm long) were center-less ground to a diameter of 1.32 cm and cut to a length of 11.0 cm. Prior to encapsulation the crystals were etched in modified CP-4 to remove surface damage and to reduce the diameter to the desired value of 1.31 cm.

The encapsulation procedure was as follows: Quartz tubes of the appropriate length were cut from stock material and the designated "cold-end" of the tube was plugged with a quartz disc, sealed and squared off. After cleaning, the cold-end graphite spacer, the etched crystal and the hot-end spacer were inserted. Subsequently a prefabricated hot-end cap with seal-off tube was fused into position with three-quarters of the ampoule immersed in cold water. The seal-off tube was then connected to a high vacuum system, the ampoule was out-gased at 200°C for 18 to 24 hours and sealed off under a pressure of 10^{-7} torr. Anchoring of the crystals near the ampoules was achieved by locally heating a small area of the ampoules near the designated cold end: InSb melted locally and the softened quartz wall deformed, (because of the reduced pressure in the sealed ampoule), anchoring the crystal into a fixed position. Figure 1A shows the individual parts of the growth assembly (as used for ground-based testing) prior to and after encapsulation.

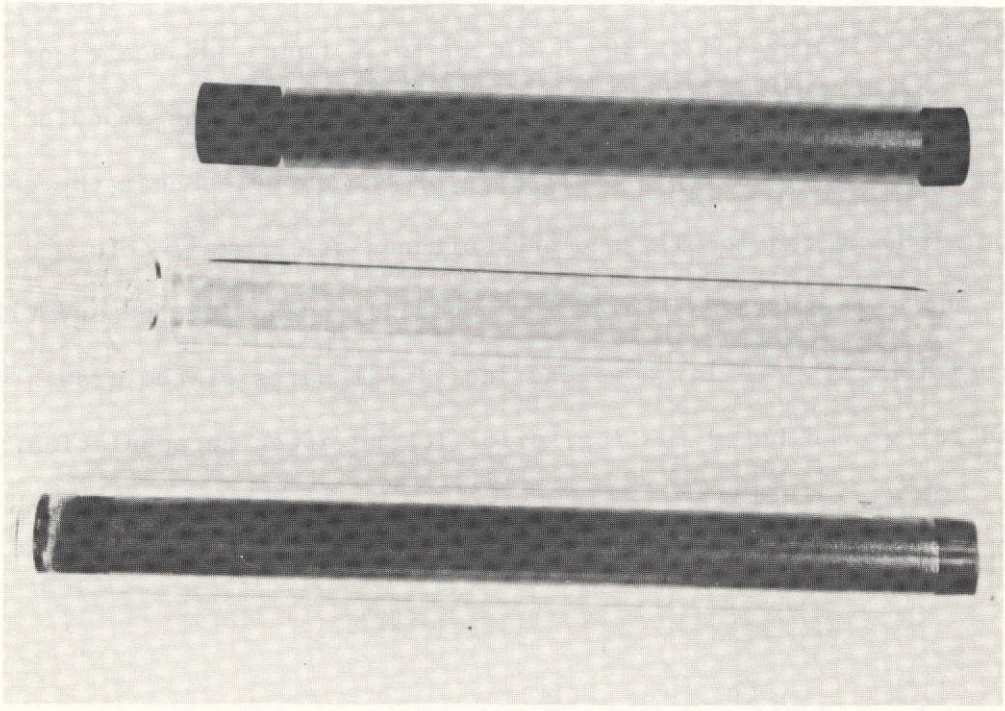

Figure 1A Crystal growth assembly (see text).

APPENDIX B

GROUND-BASED TESTING

The objectives of pre-flight testing were: (a) the optimization of characterization procedures for the study of compositional inhomogeneities on the microscale; (b) the analysis of growth and segregation behavior in confined configuration brought about by controlled power reduction (under stabilizing and destabilizing thermal gradients) and (c) the determination of the performance characteristics of the multipurpose furnace.

(a) Characterization Procedures for Compositional Inhomogeneities on the Microscale:

Extensive investigation of the resolution limits of available characterization techniques indicated the superiority of high resolution etching over electrical and mass spectrographic techniques for the detection and determination of compositional fluctuations on the microscale. The spatial resolution of the permanganate etchant (A.F. Witt, J. Electrochem Soc. 114, 298 (1967)) was significantly improved by eliminating unidirectional mechanical polishing of the InSb specimens and adopting a chemical-mechanical polisning procedure based on Syton. Optimum results were obtained by polishing the samples for 30 to 45 minutes on Corfam wheels with a Syton solution containing acetic acid (to obtain a pH of 7) and H_2O_2 (15 cm^3/litre of Syton). The etching procedure adopted is discussed in the section "Bulk Characterization".

The suitability of ion microprobe analysis for the quantitative determination of Te segregation effects on a microscale was studied using a direct imaging ion microscope (Cameca) and an ion microprobe mass analyzer (Applied Research Labs). Both techniques proved of limited value because of the extremely low yield of tellurium ionization during sputtering. The secondary Te-ion intensity was ratioed to the secondary ion intensity of the InSb matrix, a procedure which in principle should permit a reliable quantitative analysis

at the dopant concentration levels used (about 10^{18} cm^{-3}); however, the precision of the measurements could not be improved beyond ± 16%. The reduced data (concentration Te atoms/cm^3) of a longitudinal scan performed in the regrown segment (adjacent to the original regrowth interface) of the Skylab-III crystal are shown in Fig. 1B. The observed fluctuation of the measurement points is due to statistical variations and does not reflect actual fluctuations of Te concentration in the InSb matrix. The data indicate that ion microprobe scanning does not have sufficient sensitivity for the quantitative determination of microsegregation in Te-doped InSb.

In view of the limitations of the ion microprobe technique, the quantitative bulk segregation analysis was based on Hall effect measurements carried out in van der Pauw configuration. Hall effect samples (2mm x 2mm x 0.5mm) were cut from the crystals as indicated in the section Quantitative Dopant Segregation Analysis. To achieve ohmic contacts, quadrant-shaped silver films were evaporated at the four corners of each sample and the samples subsequently annealed for two hours at 350°C. Gold lead wires were soldered with indium onto the silver coated corners. The Hall effect measurements were performed in a 6" field-regulated electromagnet employing a constant current source and a calibrated, high impedance microvolt meter. To ensure a measurement precision of better than 1%, more than thirty individual Hall effect measurements (at different field strengths) were carried out on each sample. Measurements were made at 77°K and 300°K; as expected for high doping levels, it was found that the two sets of data were essentially the same.

In addition to the Te-doped crystal, the undoped crystal (grown in Skylab-III) was subjected to quantitative segregation analysis. The Hall effect data for this crystal are shown in Fig. 2B. Here, also, the steady state

segregation in space-grown crystal is achieved (after a transient region of 2.5 cm) whereas no steady state segregation is observed in the earth-grown crystal. The high carrier concentration in Skylab-III undoped crystal is apparently due to inadvertent contamination during processing on earth.

(b) Analysis of Growth and Segregation by Controlled Power Reduction in Confined Configuration:

Extensive experiments were conducted to establish the growth and segregation characteristics for InSb under stabilizing and destabilizing conditions in a vertical arrangement with a geometric configuration similar to that designed for the multipurpose furnace (see Fig. 3B). Growth experiments performed under destabilizing thermal gradients permitted for the first time the establishment of cause and effect relationships between thermal convection effects in the melt and the formation of segregation inhomogeneities in the growing crystal (K.M. Kim, A.F. Witt and H.C. Gatos, J. Electrochem. Soc. 119, 1218 (1972)). It was further shown that with decreasing melt height the growth system is successively subject to turbulent thermal convection, oscillatory thermal instability and thermal stability. From these experiments it was determined that under turbulent convection the actual microscopic growth rate (because of extensive backmelting) is by a factor of up to 20 larger than the average macroscopic growth rate and that dopant segregation is continuously subject to transient conditions to which the Burton, Prim and Slichter relationship (J.A. Burton, R.C. Prim and W.P. Slichter, J. Chem. Phys. 21, 1987 (1953)) cannot be applied. Growth experiments performed under stabilizing thermal gradients (growth in the upward direction) revealed the virtual absence of segregation inhomogeneities in the bulk of the grown crystals. In all instances, however, the single crystal matrix became polycrystalline soon after initiation of growth. The external morphology of the crystals

showed randomly distributed cavities due to out-gasing at the melting temperature of InSb. The regrown crystals exhibited a shiny surface, reflecting wetting conditions between the melt and the confining quartz ampoule.

(c) Ground-Based Tests in the Prototype of the Multipurpose Furnace:

A series of experiments were conduced in the "SIM" and prototype multipurpose furnaces to establish the required design parameters. In preliminary experiments carried out under stabilizing thermal gradients it was observed that volume redistribution of the regrown crystals resulted in fracture of the quartz ampoule. This failure led to the final design of the "hot-end" graphite spacer.

The thermal characteristics required to achieve in the multipurpose furnace an average growth of 5 μm/sec under a temperature gradient of about 20°C/cm was determined by Westinghouse on the basis of heat transfer calculations aided by temperature measurements in the "SIM" and prototype furnaces. Calculations and temperature measurements indicated a constant thermal gradient, the magnitude of which along the melt zone is a function of heat input. Temperature measurements during actual regrowth experiments showed that the thermal gradient in the melt (Fig. 4B) decreases with continuing cool-down (growth). The theoretically predicted growth rate curves, for cooling rates of 0.6°C/min and 1.2°C/min are shown in Fig. 5B. The data indicate a steady increase in growth rate with average values of about 5.5 μm/sec and 3.0 μm/sec for cooling rates of 1.2 and 0.6°C/min, respectively (for a four-hour cool-down period).

To verify the actual growth rate in the multipurpose furnace a cartridge assembly was modified to permit interface demarcation during growth (M. Lichtensteiger, A.F. Witt and H.C. Gatos, J. Electrochem. Soc. 118, 1013 (1971)) under

stabilizing thermal gradients by transmitting during regrowth current pulses (18A) of 50 msec duration at intervals of 2 seconds across the growth interface. The analysis was carried out by cutting the regrown crystal along the regrowth axis, polishing the exposed (211) plane and etching it. The microscopic growth rate data were obtained by measuring under the microscope the spacings of consecutive demarcation lines. Fig. 6B shows the measured microscopic growth rate behavior associated with a cool-down rate of 1.17°C/min. The measurements indicate a significant discrepancy with the theoretical growth rate curve: while the average growth rate is in good agreement with that predicted, the actual microscopic growth rate assumes a constant value over about 60% of the regrown region. This particular behavior is attributed to the presence of slow laminar convective flow established in the melt as a consequence of unavoidable, radial thermal gradients which are destabilizing in the presence of gravitational forces; convection in turn tends to reduce existing thermal gradients and thus is a stabilizing influence on the prevailing microscopic growth rate. The experimental growth rate data confirm in principle the theoretically predicted growth behavior, since it must be assumed that destabilizing conditions are not encountered under zero gravity conditions in space.

The experimental results indicate clearly that it is virtually impossible to achieve on earth homogeneous, steady state segregation since unavoidable radial thermal gradients result in thermal convection which prevents the effective segregation coefficient from reaching unity.

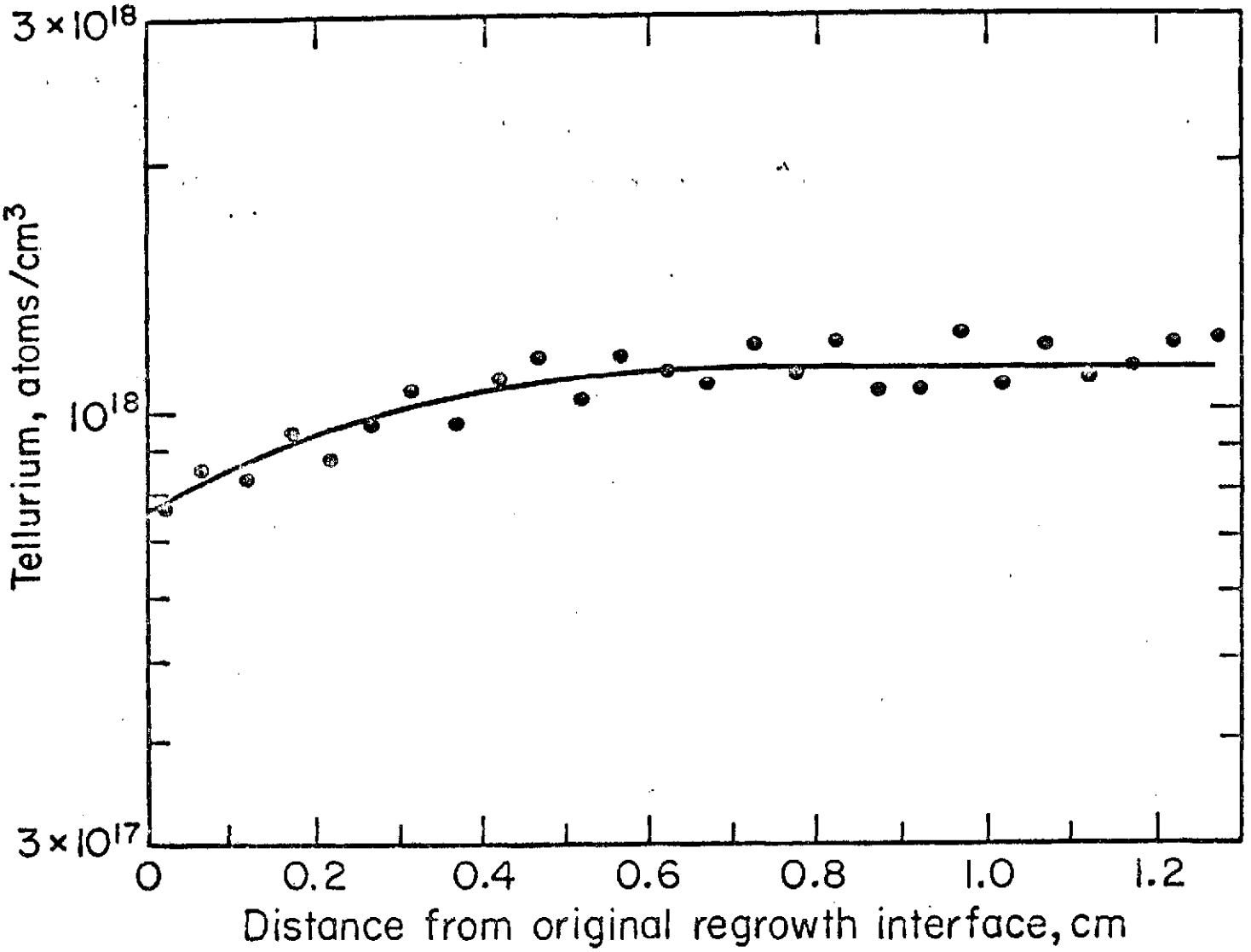

Figure 1B Longitudinal ion microprobe scan on the Te-doped crystal grown in Skylab-III.

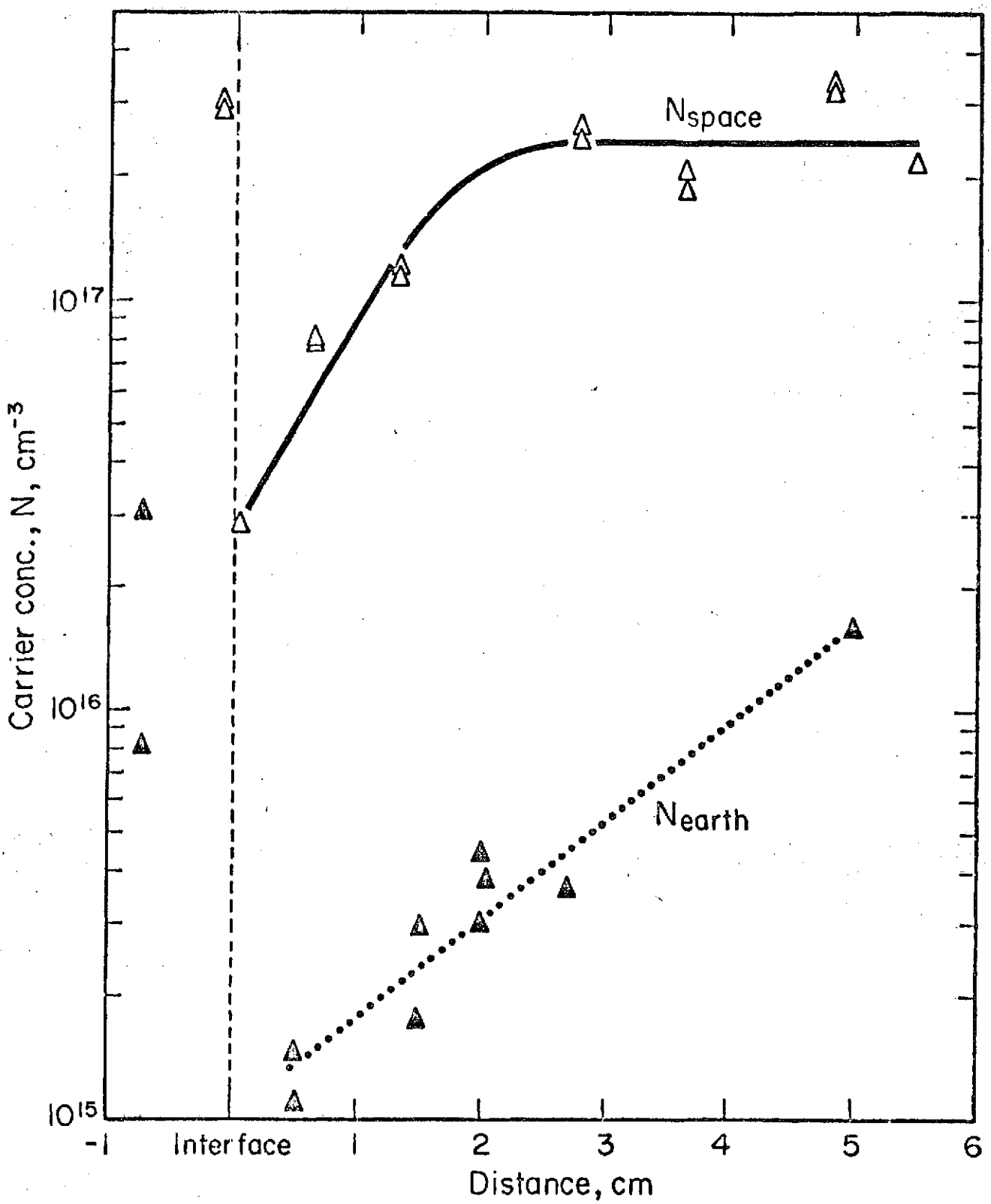

Figure 2B Carrier (dopant) concentration profile obtained from Hall-effect measurements for undoped crystal grown in Skylab-III (N_{space}) and in ground-based testing (N_{earth}).

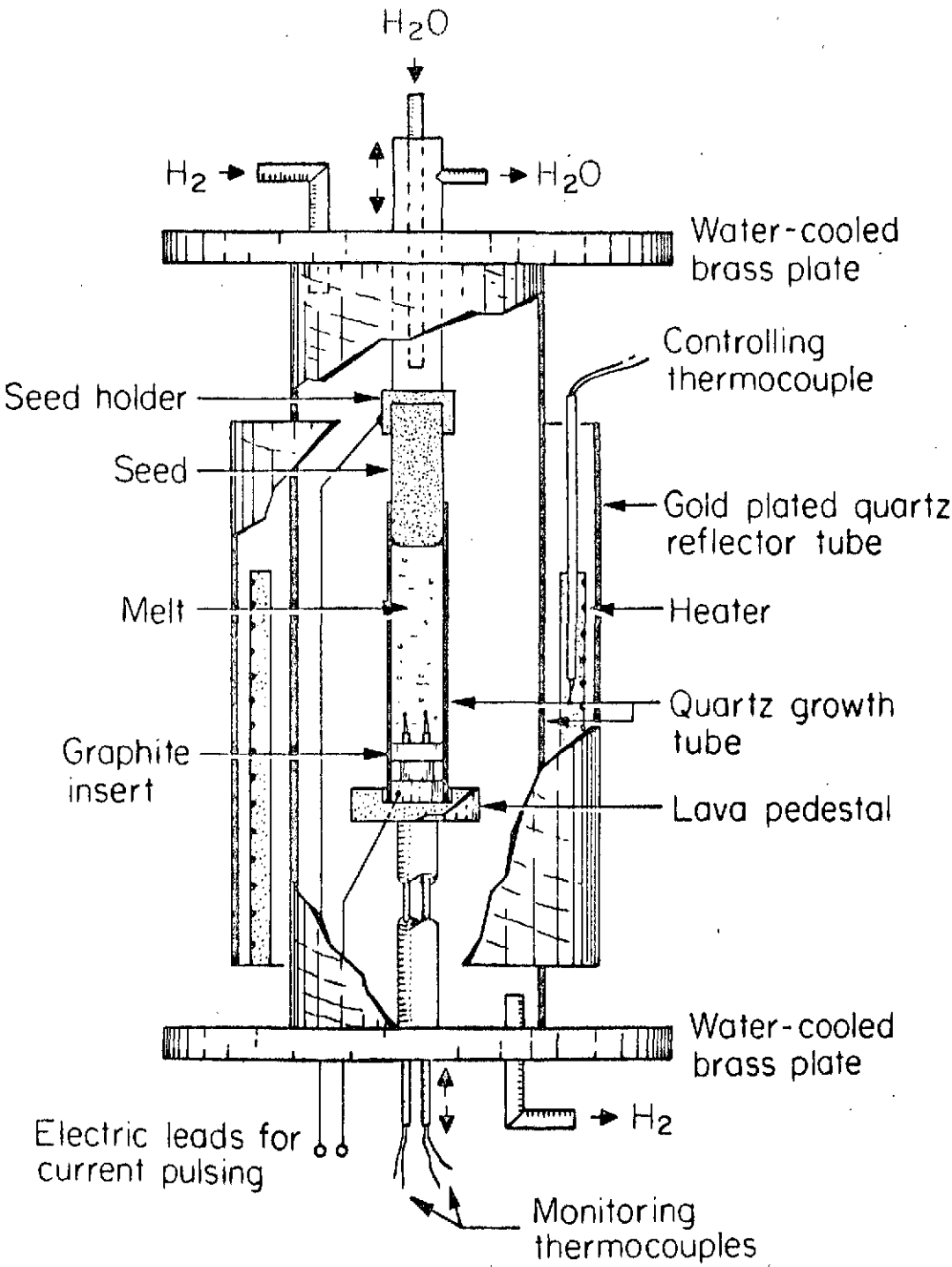

Figure 3B Schematic diagram of the apparatus used for the study of crystal growth under destabilizing (as shown) and stabilizing thermal gradients.

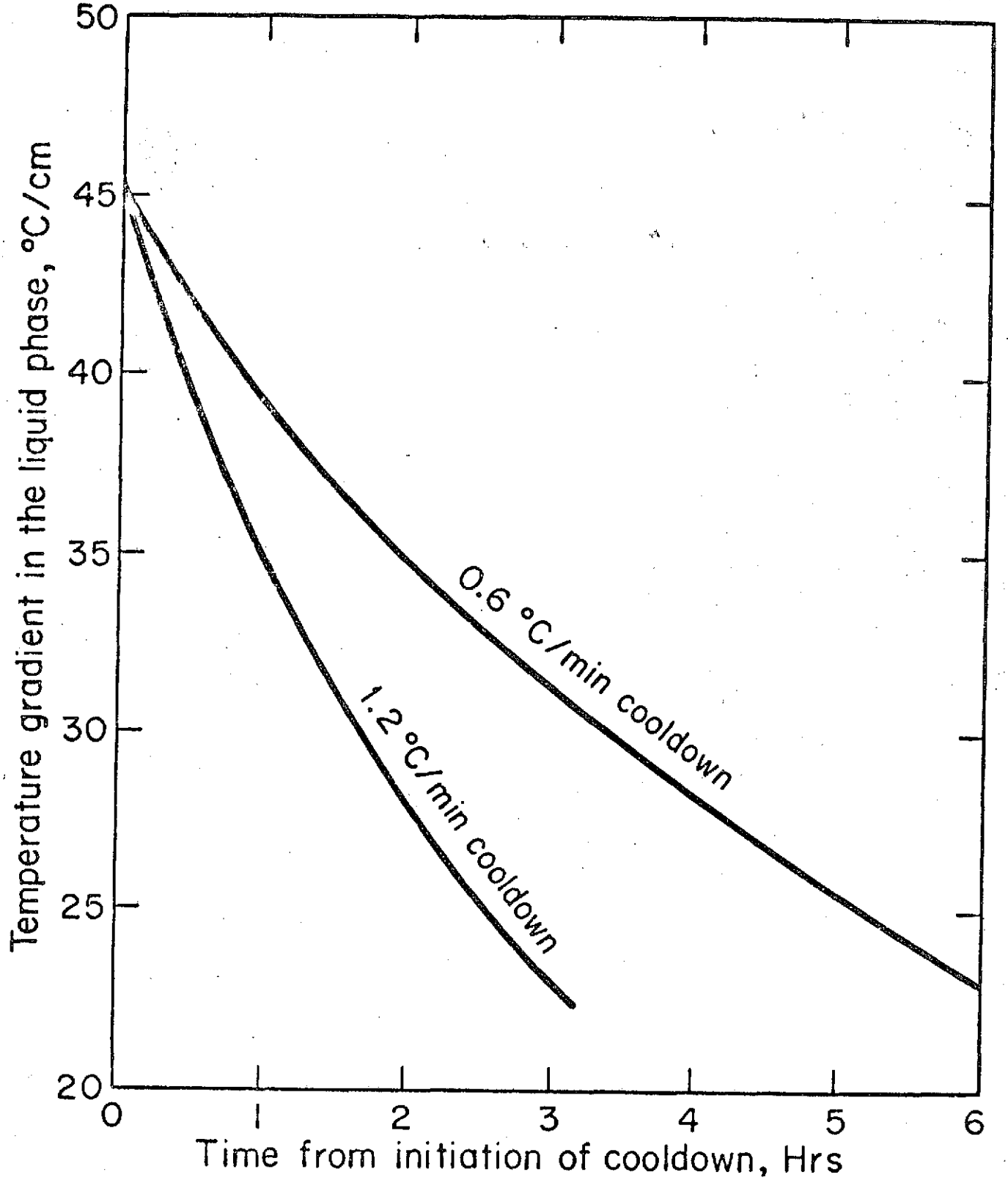

Figure 4B Temperature measurements during growth experiments (on earth) in multipurpose furnace showing that thermal gradient in the melt decreases with continuing solidification.

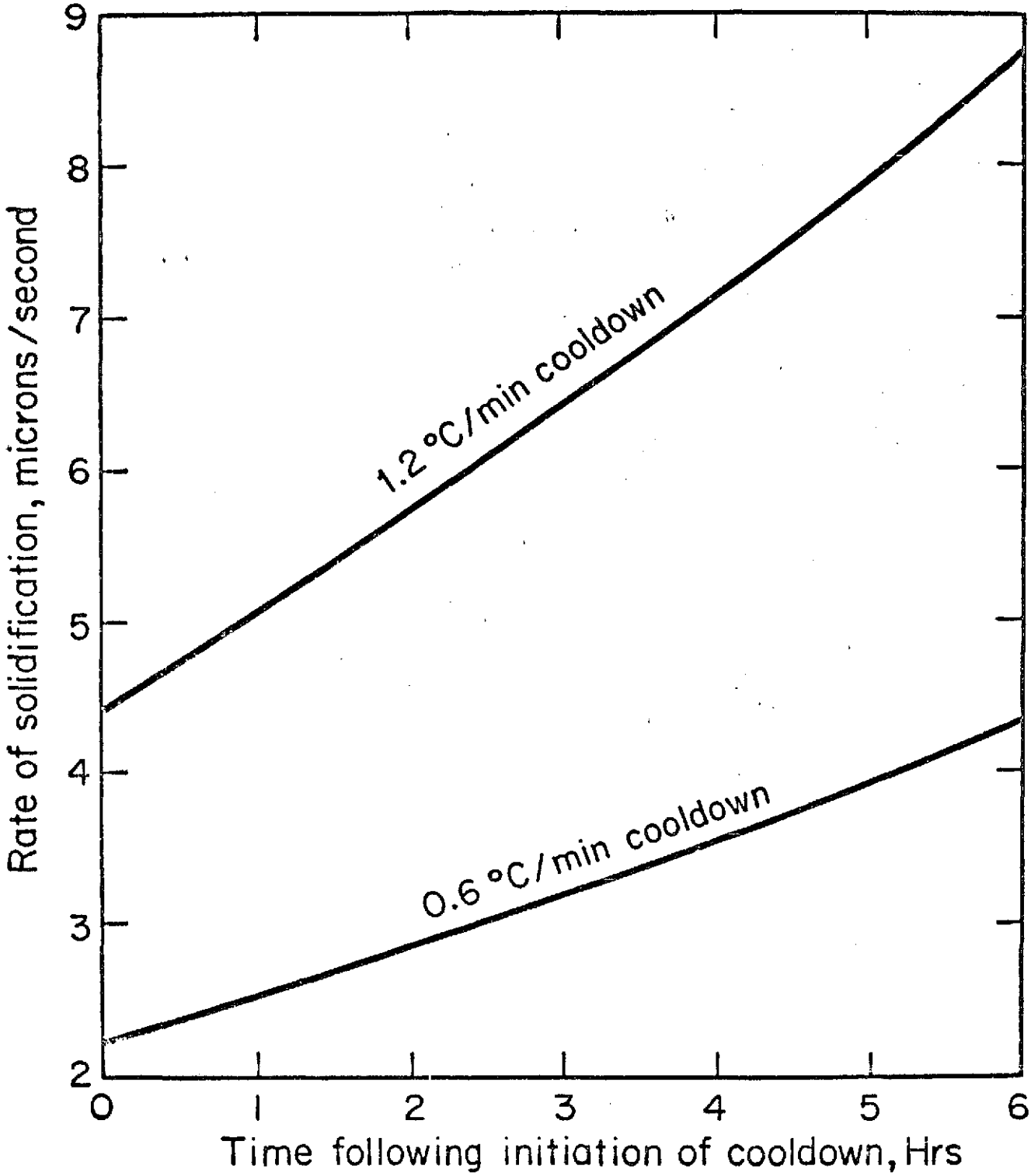

Figure 5B Theoretically predicted growth rates for cooling rates of 0.6°C/min and 1.2°C/min.

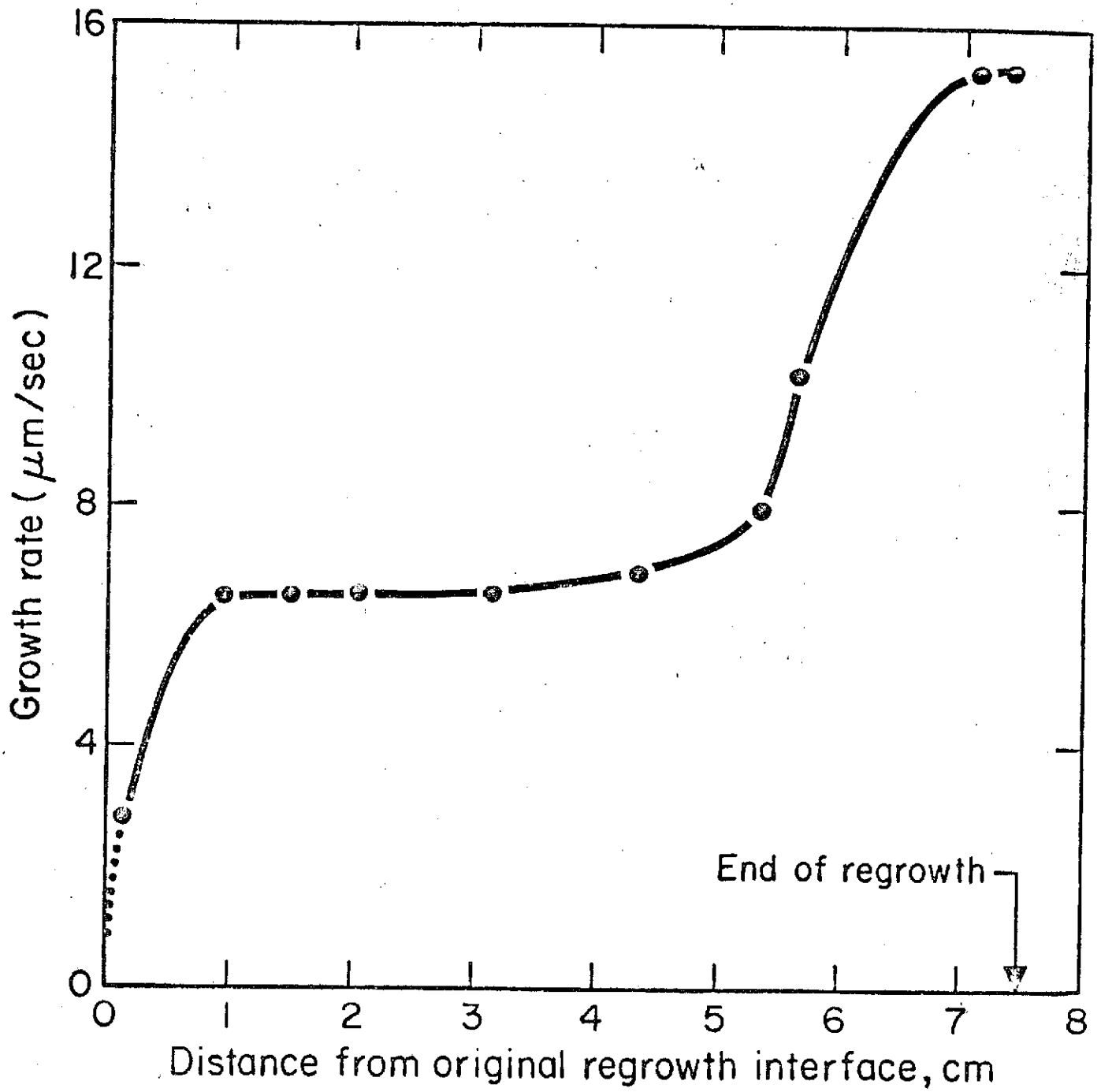

Figure 6B Microscopic growth rate measurements in ground-based experiment with cool-down rate of 1.17°C/min.

APPENDIX C

SUPPLEMENTARY INFORMATION

The salient findings in the InSb growth Skylab experiments and the significant conclusions drawn from these findings are discussed in the bulk of the report. Relevant details pertaining to experimental techniques, procedures and materials are presented in the preceding appendices.

This appendix contains miscellaneous observations which are either in themselves of interest or reflect phenomena and effects which could not be pursued further in the context of the present experiment. They are included here in the interest of maintaining the coherence of the bulk of the report.

Figure 1C is a radiograph of the three Skylab-III crystals through the steel cartridges after return to Marshall Space Flight Center; regrowth in space took place downwards; the undoped crystal is to the right, the Te-doped is at the center, and the Sn-doped at the left.

The same crystals (as in Figure 1C) photographed through the quartz ampoules are shown in Figure 2C (1.5X); the regrowth interface is at the left-hand side of each crystal; the heavily Sn-doped crystal is at the bottom, the Te-doped is in the middle and the undoped crystal is at the top of the figure.

Figure 3C (2X) shows the three crystals grown in Skylab-IV, the arrangement of these crystals is as in Figure 2C.

The Sn-doped crystal grown in Skylab-III is shown in Figure 4C (2X) before removing it from the ampoule (regrowth interface toward bottom of figure); note Sn phase along the crystal (bright spots) and Sn extrusion into the cavity of the hot-end graphite spacer; the original crystal was intentionally heavily

doped to attain constitutional supercooling (interface breakdown) during regrowth in space.

Figure 5C (3X) shows the hot-end of the ampoule containing the Te-doped crystal grown in Skylab-IV; the polycrystalline material extruded into the cavity of the graphite spacer during the final stages of solidification is clearly shown in this figure.

Figure 6C (.9X) shows a Sn-doped crystal removed from its ampoule by cutting the ampoule longitudinally after ground-based testing; because of wetting, detaching of the crystal from the quartz was not feasible without damaging the crystal, accordingly, this method of removing the crystals from the ampoules was abandoned; all Skylab-grown crystals were removed by dissolving the ampoules in 48% HF.

Figure 7C (8.5X) shows the end (solidified in contact with the graphite spacer) of the undoped crystal grown in Skylab-III; the oval shape of this end reflects the radial thermal asymmetry prevailing during crystal growth; this type of asymmetry was observed on all crystals grown in space (this asymmetry could not be observed in the cases where extrusion took place into the cavity of the hot-end spacer).

Ridges and patterns observed on the as-grown surface of the Te-doped crystal (Skylab-IV) are shown in Figure 8C (150X).

A ridge configuration towards the end of the Te-doped crystal grown in Skylab-III is shown in Figure 9C (200X); note that the ridges have become flat and are of relatively uniform height (approximately 25 μm).

The surface morphology, between ridges, of the Te-doped crystal (Skylab-III) is seen in Figure 10C (200X). The patterns seen on the surface do not propagate into the bulk of the crystal as seen in Figure 11C (200X) where a

polished and etched cross-section of the crystal is shown (light portion of figure).

Figure 12C (10X) is a double beam interferogram of an etched cross-section of the crystal grown in Skylab-III; the space-grown segment is on the left-hand side and the seed on the right-hand side of the figure; note that in the earth-grown segment the compositional inhomogeneities are revealed as deflections of the fringes; no such deflections are seen in the space-grown segment; the abrupt fringe deflection at the regrowth interface indicates the segregation transient during the initial stages of regrowth; subsequently the space-grown segment exhibits compositional homogeneity on a macroscale.

Pronounced peripheral faceting in the regrowth segment of a ground-based experiment (Te-doped crystal) is shown in Figure 13C (450X); growth took place from right to left.

Figure 14C (5X) shows cross-sections of the undoped crystal grown in Skylab-III; the increase in dislocation density and peripheral twinning is seen as regrowth advances; (a) seed section about 0.2 cm from the regrowth interface; (b) space-grown section approximately 1.8 cm beyond regrowth interface; (c) section approximately 3.8 cm beyond interface; (d) section approximately 5.6 cm beyond interface.

In Figure 15C (125X) two photomicrographs (under dark field illumination) of the peripheral areas of a cross-section of the undoped crystal grown in Skylab-III are shown; the two sections include the interface between the seed and the space-grown crystal where the melt contacted the quartz wall of the ampoule; the dislocation patterns reflect the strain induced by the constraint of the wall upon solidification (InSb expands approximately 13% upon freezing).

Both types of dislocations (alpha and beta) expected to be present in InSb are seen on a cross-section of the Te-doped crystal grown in Skylab-IV shown in Figure 16C (200X); large pits correspond to beta dislocations.

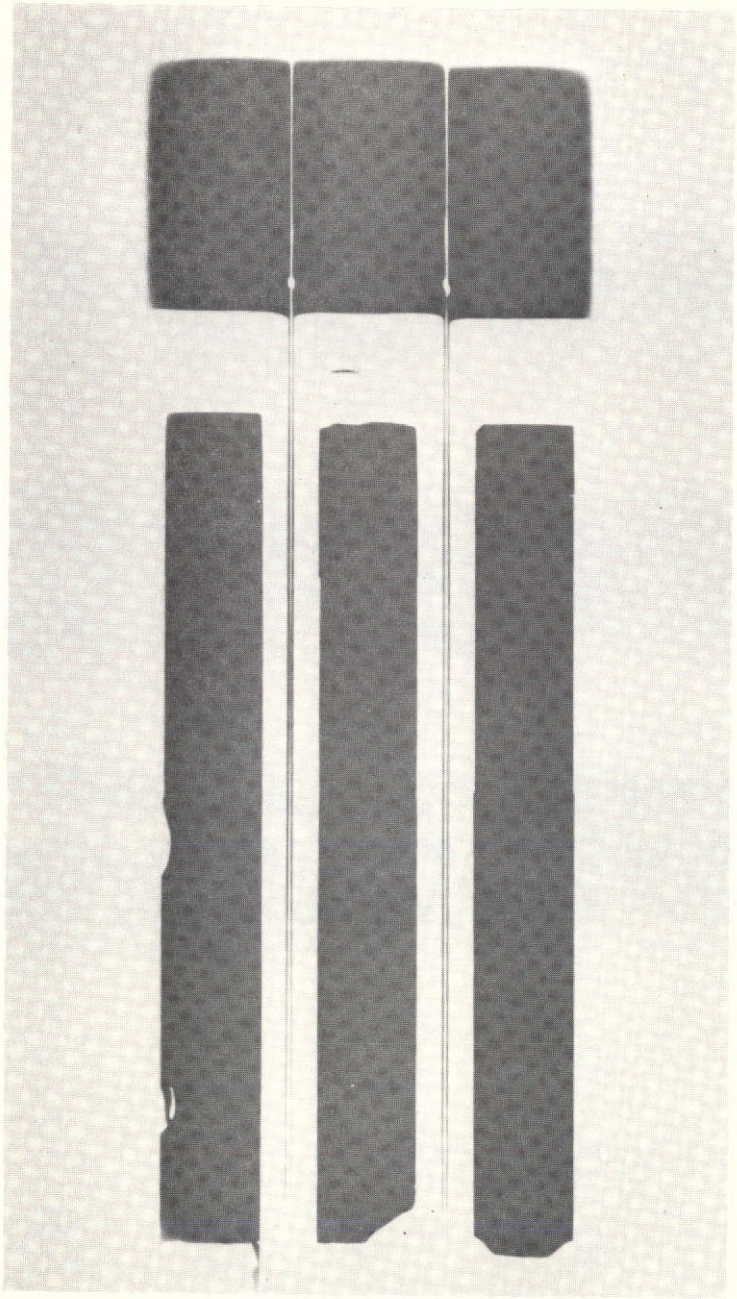

Figure 1C

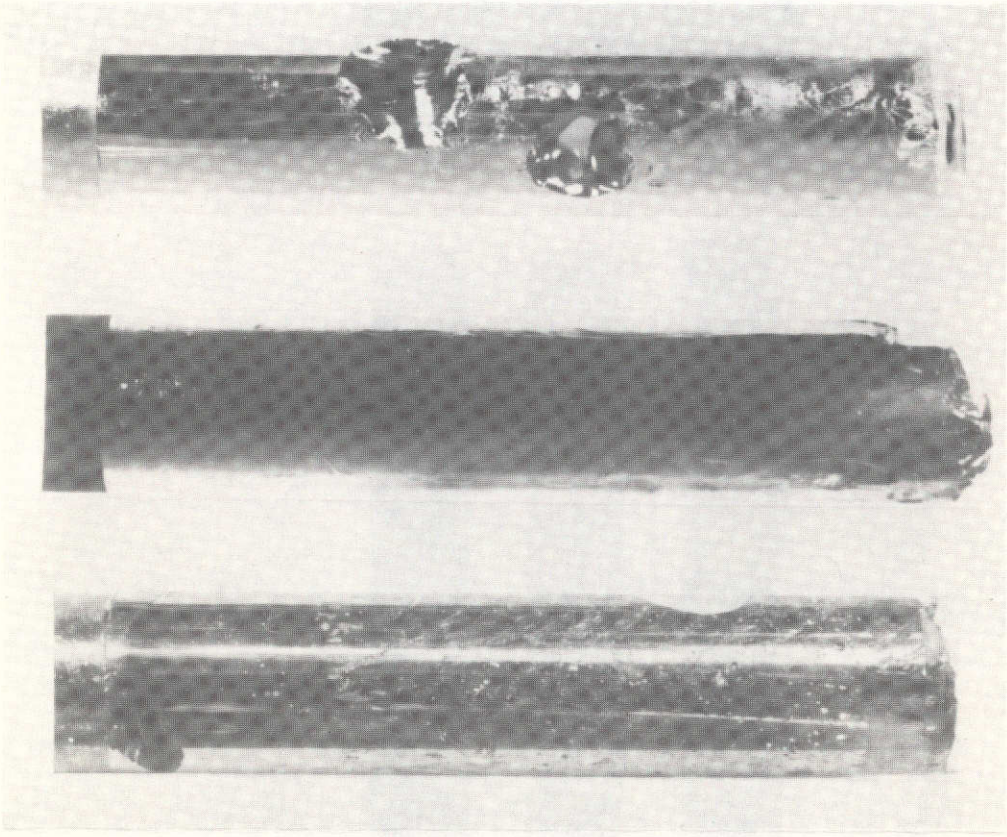

Figure 2C

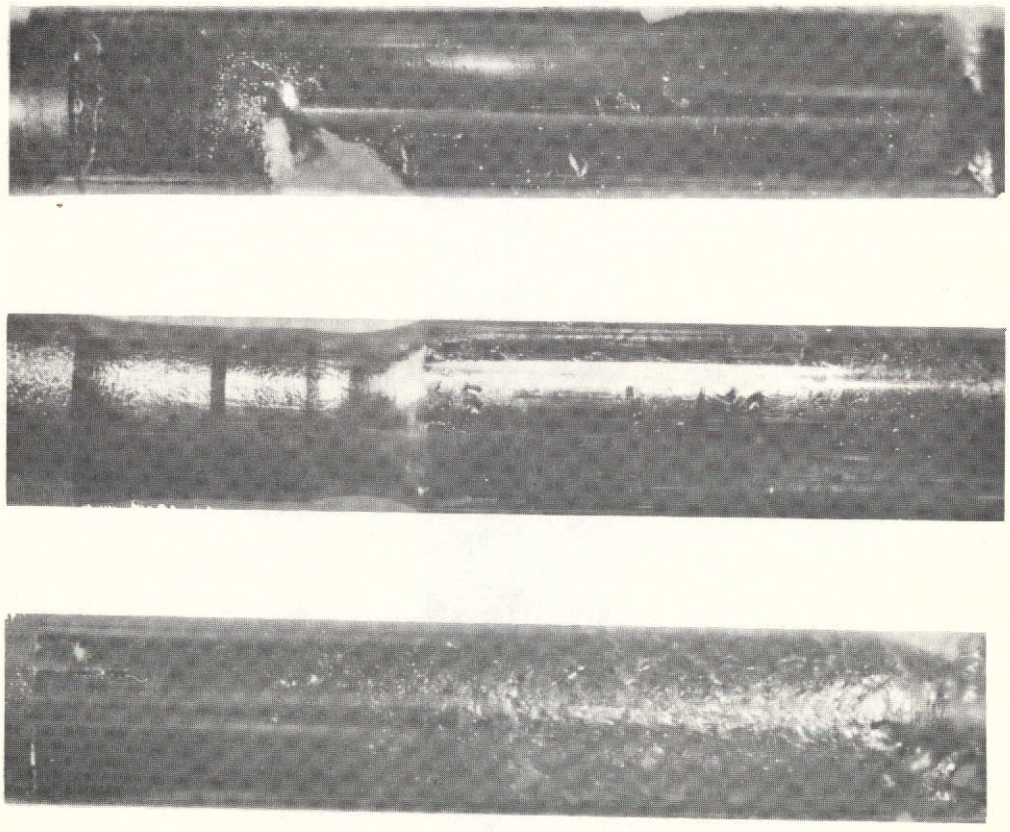

Figure 3C

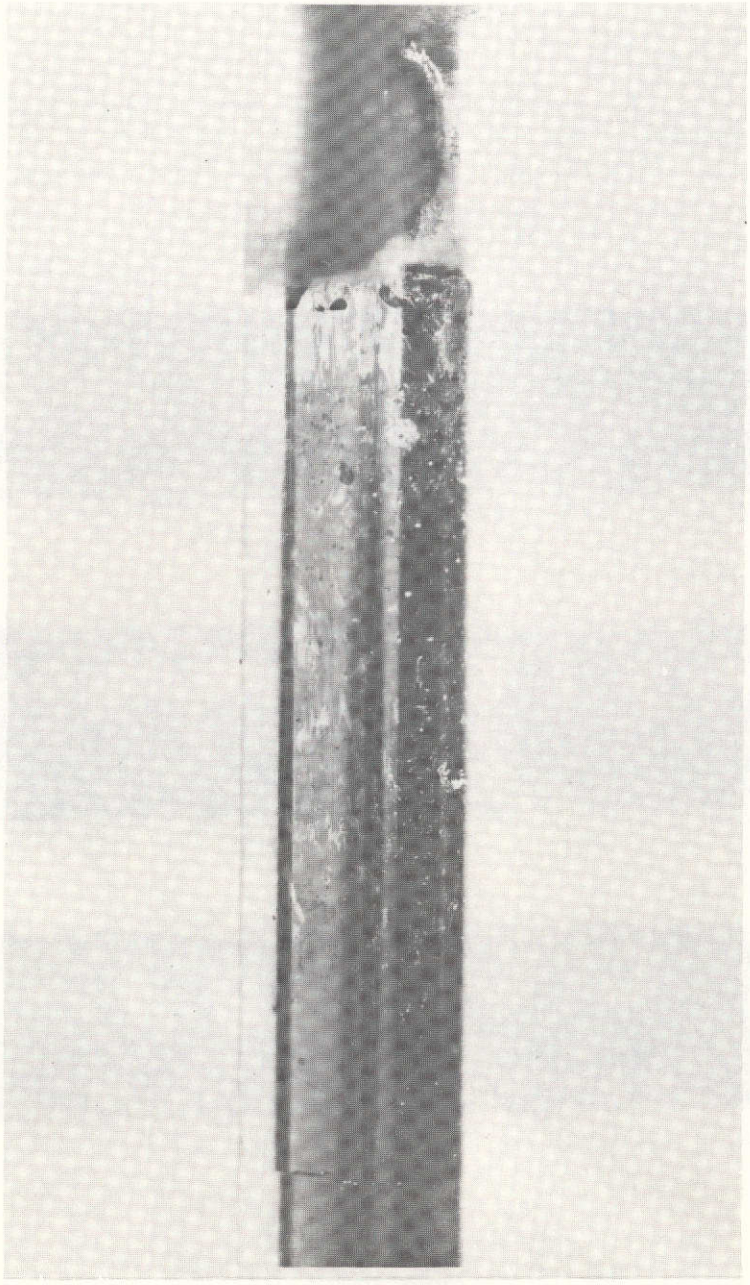

Figure 4C

Figure 5C

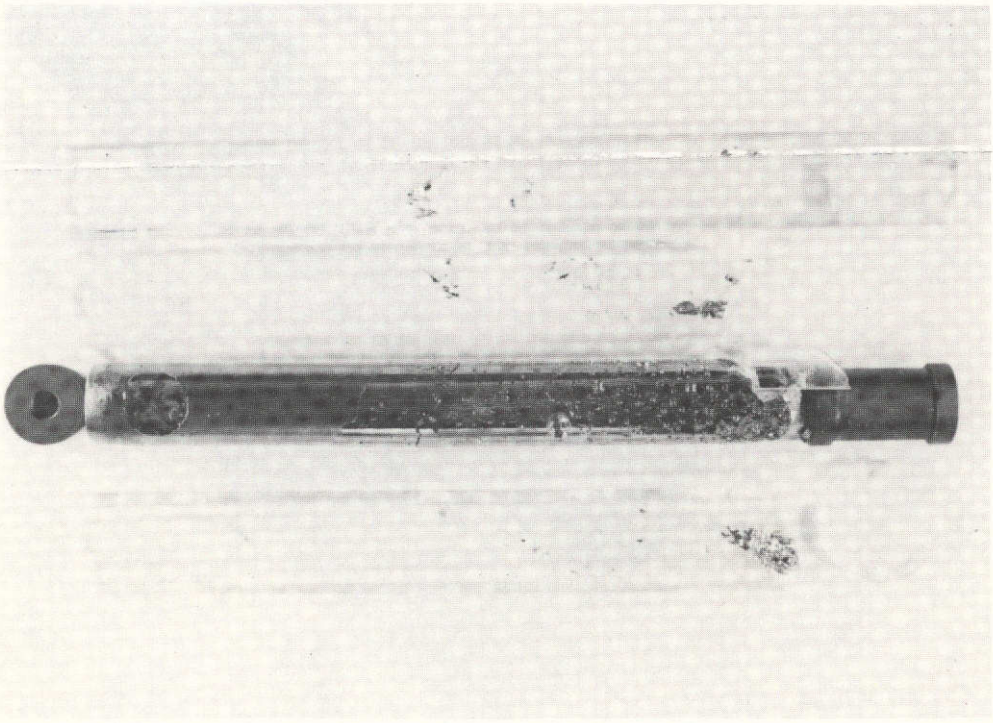

Figure 6C

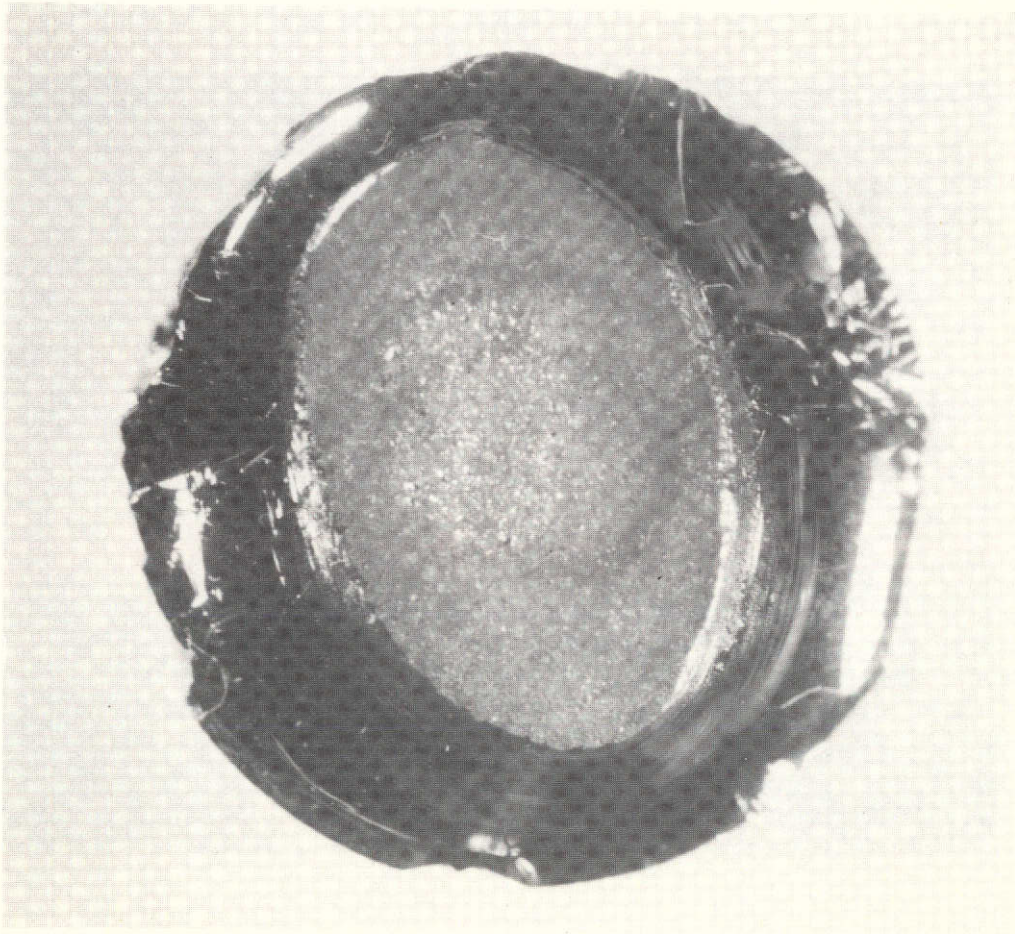

Figure 7C

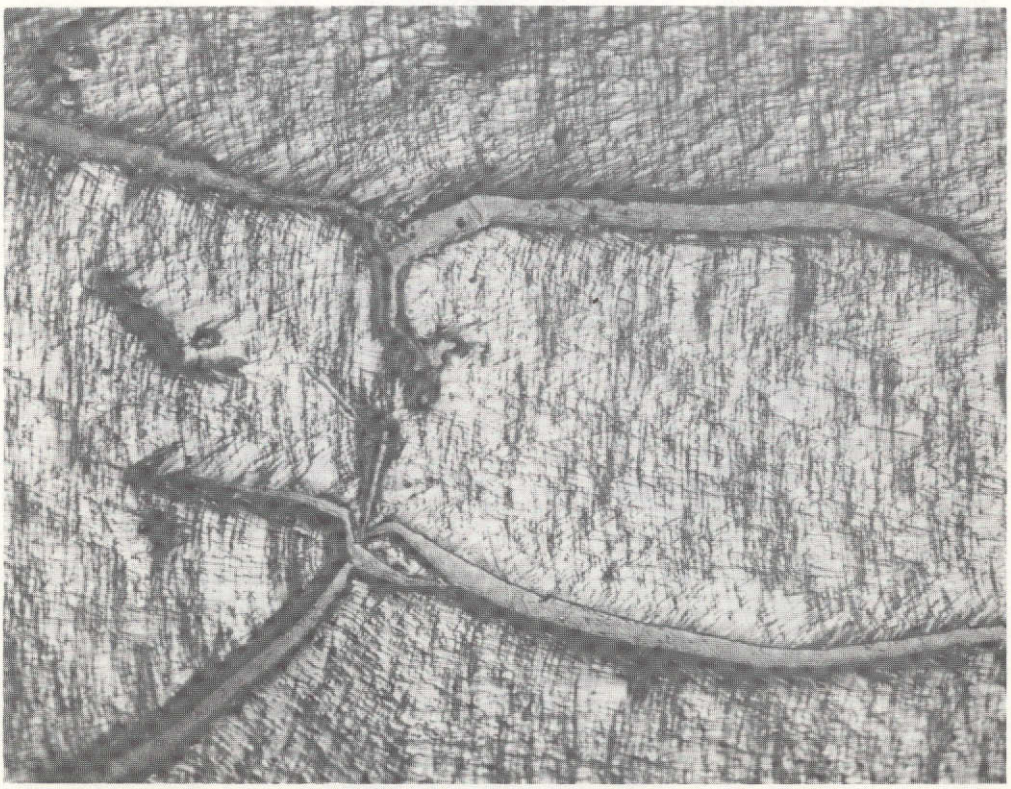

Figure 8C

Figure 9C

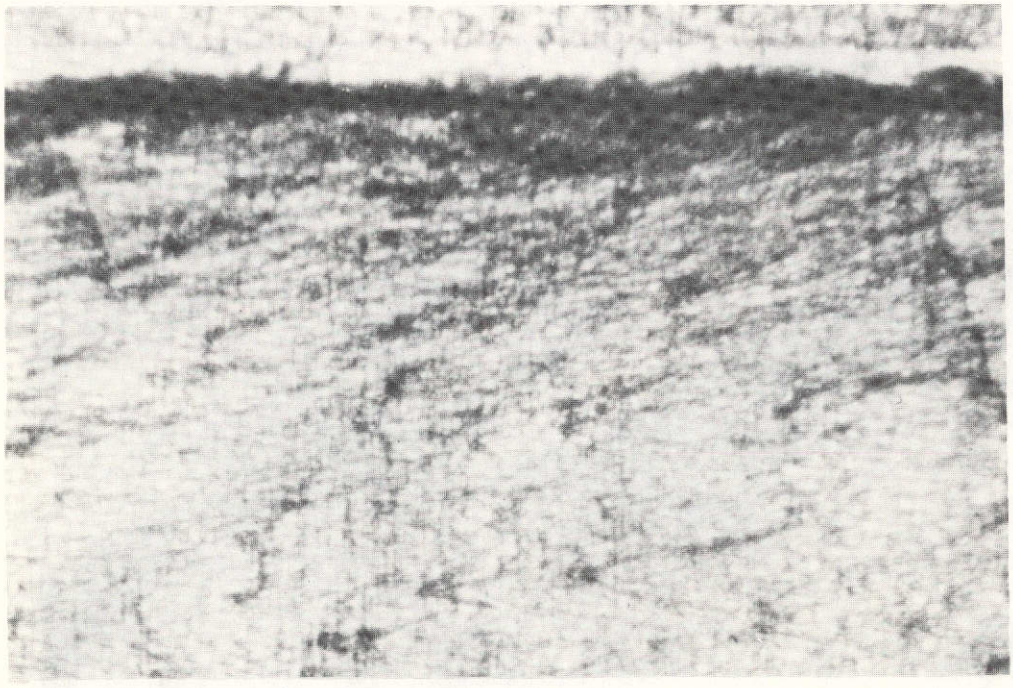

Figure 10C

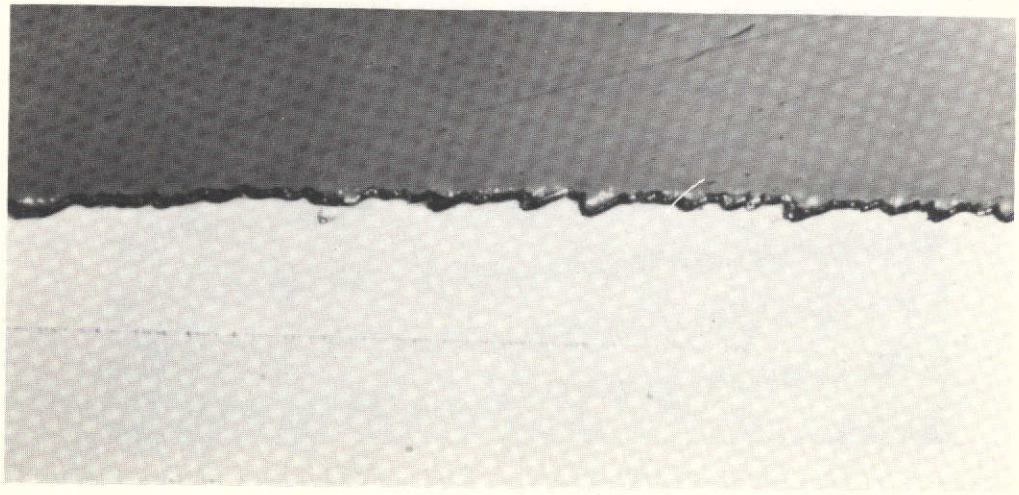

Figure 11C

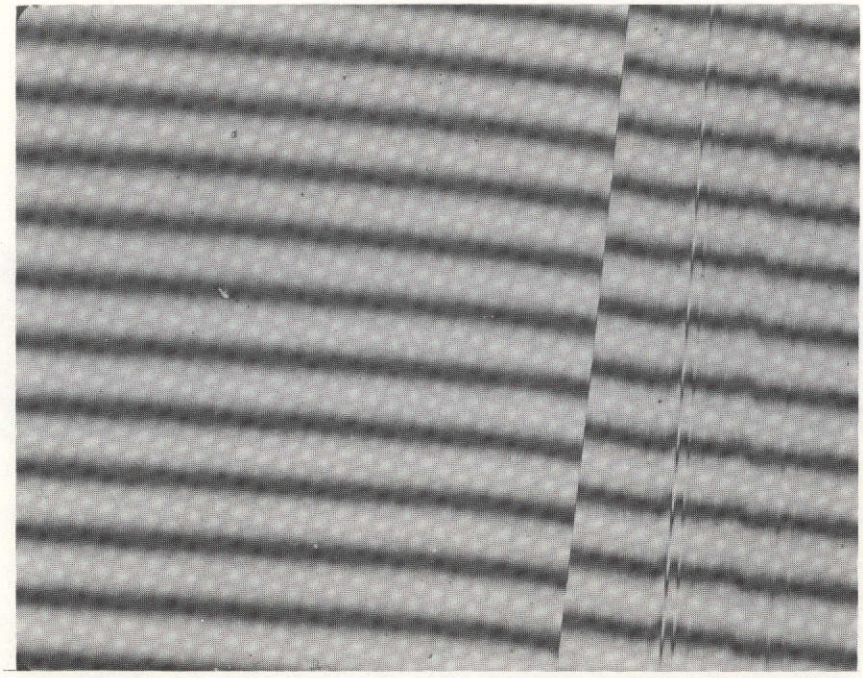

Figure 12C

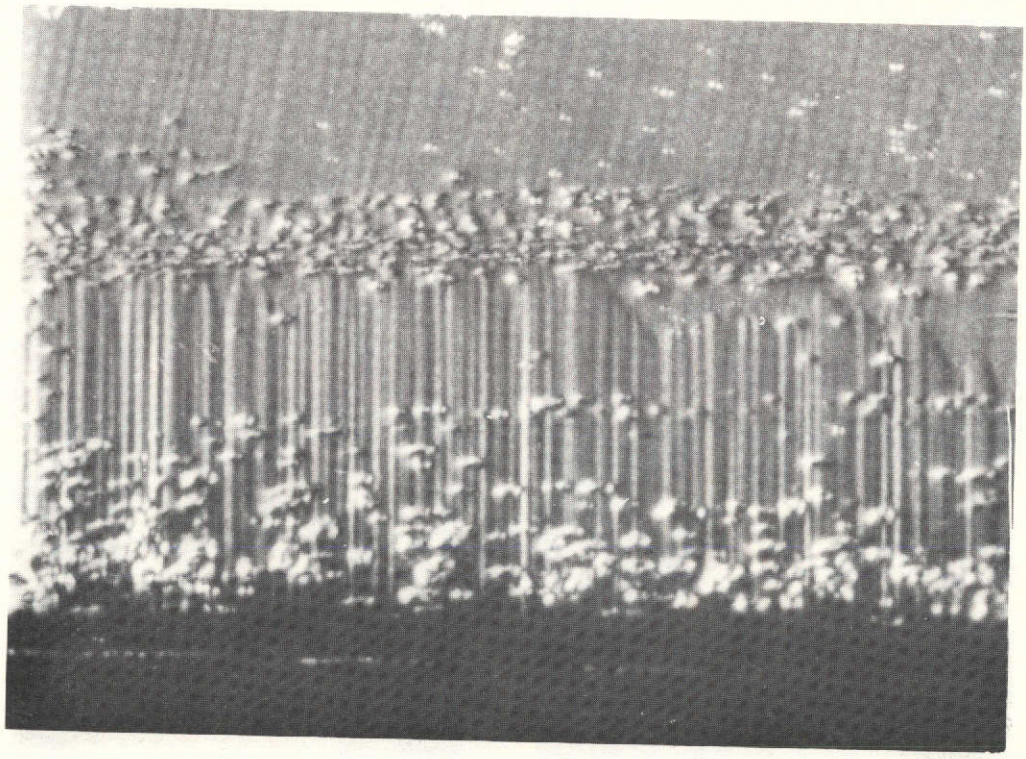

Figure 13C

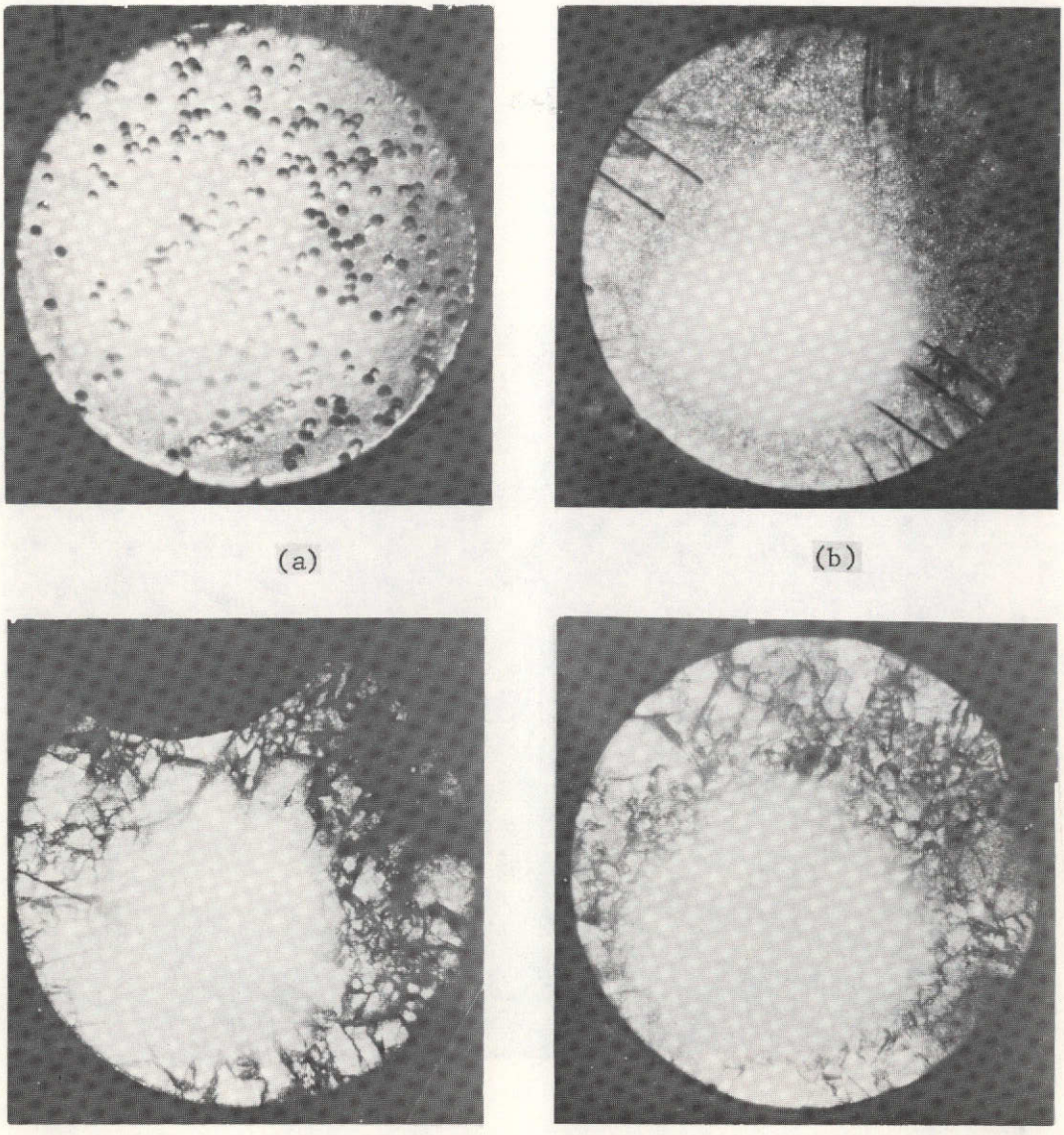

(a) (b)

(c) (d)

Figure 14C

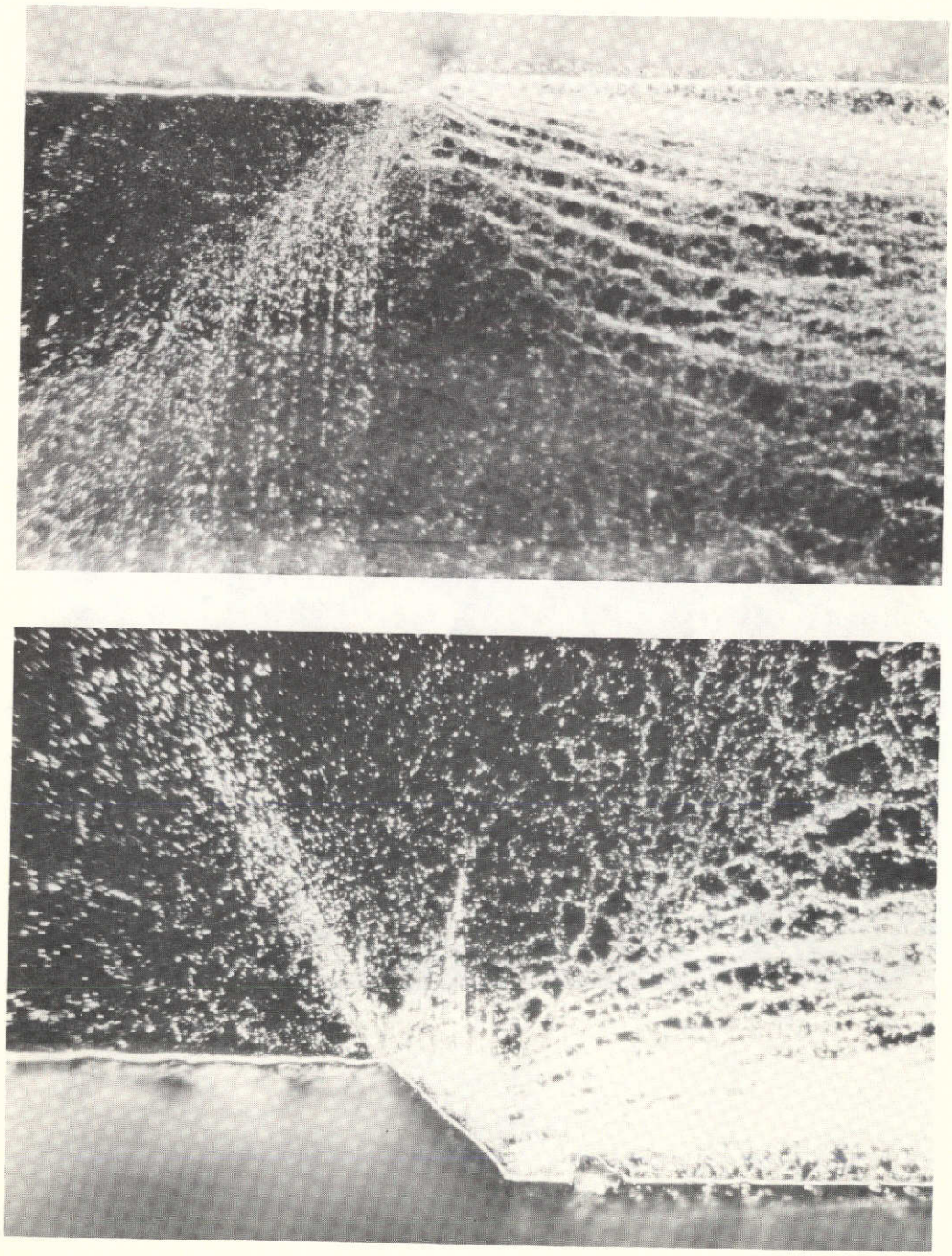

Figure 15C

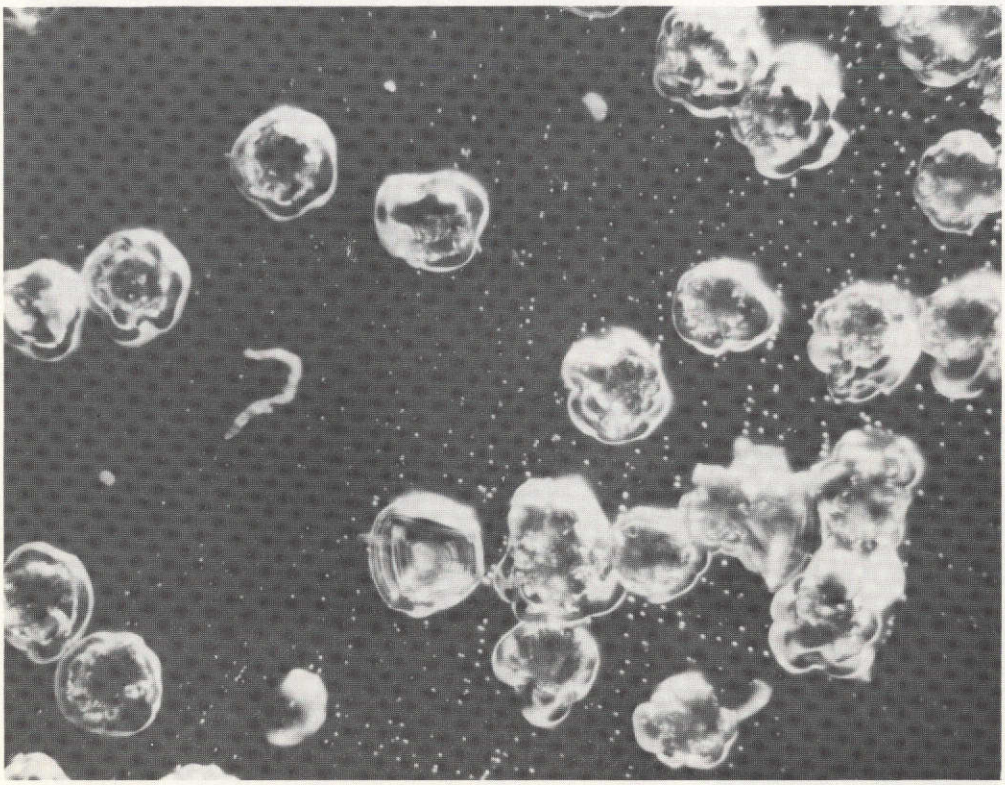

Figure 16C

☆U.S. GOVERMENT PRINTING OFFICE 1975—640-450/185 REGION NO. 4